

Low-Valent Ruthenium Complexes of the Non-innocent
2,6-Bis(imino)pyridine LigandMichelle Gallagher, Noah L. Wieder, Vladimir K. Dioumaev, Patrick J. Carroll, and
Donald H. Berry*

Department of Chemistry, University of Pennsylvania, Philadelphia, Pennsylvania 19104-6323

Received October 14, 2009

A series of low-valent ruthenium complexes bearing 2,6-bis(imino)pyridyl (“[N₃”]) ligands has been synthesized and characterized. Reduction of [N₃]RuCl₂(C₂H₄) ([N₃^{xy1}] = 2,6-(XylNCMe)₂-C₅H₃N, **1a**; [N₃^{mes}] = 2,6-(MesNCMe)₂C₅H₂N, **1b**; [t-Bu-N₃^{mes}] = 2,6-(MesNCMe)₂p-^tBuC₅H₂N, **1c**) with hydridosilanes in an arene solvent such as toluene yields new 18e⁻ η⁶-arene complexes [κ²-N₃]Ru(η⁶-MeC₆H₅), **2a,b,c**, in which the [N₃] ligand is bidentate and only one imine group is coordinated to the metal. The arene ligand can be displaced with dinitrogen in non-arene solvents to yield the binuclear, four-coordinate, formally Ru(0) complexes {[N₃]Ru}₂(μ-N₂), **3a,b,c**. Pyrophoric complex **3c** is a rare example of a structurally characterized Ru(0) dinitrogen complex. Treatment of low-valent complexes **2** or **3** with donor ligands generates five-coordinate complexes [N₃^{xy1}]RuL_{1,2} (L_{1,2} = C₂H₄, **4a**; L_{1,2} = PMe₃, **5a**; L_{1,2} = CO, **6a**; L₁ = PMe₃, L₂ = CO, **7a**). Complexes **2a**, **3c**, **5a**, **6a**, and **7a** are diamagnetic and have been structurally characterized by single-crystal X-ray diffraction methods. New six-coordinate Ru(II) complexes [N₃^{xy1}]RuCl₂(L) (L = PMe₃, CO) were also isolated and structurally characterized. The infrared data, observed geometrical parameters, and reactivity patterns of the formally Ru(0) centers suggest varying degrees of electron delocalization to the “non-innocent” bis(imino)pyridyl, but probably not to the extent implied by the valence tautomeric [N₃]²⁻/Ru(II) canonical form. Although the [N₃]⁻/Ru(I) representation may portray the electron distribution more accurately than “Ru(0)”, the inherent odd electron counts on both ligand and metal—and requisite antiferromagnetic coupling—provides little in the way of “useful” distinctions or predictive value for the low-valent [N₃]Ru(L)₂ complexes with strong-field co-ligands such as CO and PMe₃. These five-coordinate adducts seem to be adequately described as Ru(0) complexes of the neutral [N₃] ligand. However, “non-innocent” valence tautomeric canonical forms such as [N₃]⁻/Ru⁺ may be more applicable to the four-coordinate dinitrogen complexes {[N₃]Ru}₂(μ-N₂).

Introduction

Over the past decade, late transition metal complexes bearing 2,6-bis(imino)pyridyl ligands, [N₃], and other

pincer-type ligands have gained attention due to their use in catalysis and in other chemical transformations.^{1–5} For example, bis(imino)pyridyl complexes of Ni, Pd, Fe, and Co are effective catalysts for the polymerization of ethylene,^{1b–h} and [N₃] complexes of ruthenium in particular catalyze a variety of reactions, including cyclohexene epoxidation² and cyclopropanation of styrene.³ Chirik and co-workers have also demonstrated that [N₃]Fe complexes catalyze reactions such as hydrogenation, hydrosilylation, and [2π + 2π] cycloaddition reactions.⁴ These ligands and other similar pincer complexes have thus emerged as a convenient and synthetically flexible alternative to the well-studied 2,2':6',2''-terpyridine (terpy) ligand.^{5–7}

Tridentate bis(imino)pyridyl ligands enforce the *mer* geometry that has been found to promote catalytic activity in

*Corresponding author. E-mail: berry@sas.upenn.edu.

(1) (a) Gibson, V. C.; Redshaw, C.; Solan, G. A. *Chem. Rev.* **2007**, *107*, 1745–1776. (b) Ittel, S. D.; Johnson, L. K.; Brookhart, M. *Chem. Rev.* **2000**, *100*, 1169–1203. (c) Paulino, I. S.; Schuchardt, U. *Catal. Commun.* **2004**, *5*, 5–7. (d) Chen, Y.; Chen, R.; Qian, C.; Dong, X.; Sun, J. *Organometallics* **2003**, *22*, 4312–4321. (e) Britovsek, G. J. P.; Bruce, M.; Gibson, V. C.; Kimberley, B. S.; Maddox, P. J.; Mastroianni, S.; McTavish, S. J.; Redshaw, C.; Solan, G. A.; Strömberg, S.; White, A. J. P.; Williams, D. J. *J. Am. Chem. Soc.* **1999**, *121*, 8728–8740. (f) Small, B. L.; Brookhart, M. *J. Am. Chem. Soc.* **1998**, *120*, 7143–7144. (g) Small, B. L.; Brookhart, M.; Bennett, A. M. *J. Am. Chem. Soc.* **1998**, *120*, 4049–4050. (h) Bouwkamp, M. W.; Lobkovsky, E.; Chirik, P. J. *J. Am. Chem. Soc.* **2005**, *127*, 9660–9661.

(2) Cetinkaya, B.; Cetinkaya, E.; Brookhart, M.; White, P. S. *J. Mol. Catal. A* **1999**, *142*, 101–112.

(3) Bianchini, C.; Lee, H. M. *Organometallics* **2000**, *19*, 1833–1840.

(4) (a) Bart, S. C.; Lobkovsky, E.; Chirik, P. J. *J. Am. Chem. Soc.* **2004**, *126*, 13794–13807. (b) Bart, S. C.; Lobkovsky, E.; Bill, E.; Chirik, P. J. *J. Am. Chem. Soc.* **2006**, *128*, 5302–5303. (c) Archer, A. M.; Bouwkamp, M. W.; Cortez, M.-P.; Lobkovsky, E.; Chirik, P. J. *Organometallics* **2006**, *25*, 4269–4278. (d) Bouwkamp, M. W.; Bowman, A. C.; Lobkovsky, E.; Chirik, P. J. *J. Am. Chem. Soc.* **2006**, *128*, 13340–13341.

(5) Van der Boom, M. E.; Milstein, D. *Chem. Rev.* **2003**, *103*, 1759–1792.

(6) Abbenhuis, R. A. T. M.; del Rio, I.; Bergshoef, M. M.; Boersma, J.; Veldman, N.; Spek, A. L.; van Koten, G. *Inorg. Chem.* **1998**, *37*, 1749–1758.

(7) Thompson, A. M. W. C. *Coord. Chem. Rev.* **1997**, *160*, 1–52.

certain ruthenium phosphine complexes.⁸ For example, we have previously reported that the active catalytic species for dehydrocoupling of silanes to carbosilanes are $16e^-$ $(\text{PMe}_3)_3\text{Ru}(\text{SiR}_3)(\text{R})$ complexes ($\text{R} = \text{H}$ or alkyl) with the meridional geometry.^{8,9} These complexes undergo facile, productive intra- and intermolecular addition of H–H, Si–H, C–H, and Si–C bonds, leading to C–H activation and functionalization. Similarly, *mer*-(PMe_3)₃Ru(GeR_3)₂ ($\text{R} = \text{alkyl}$ or aryl), generated by phosphine loss from the tetrakis-phosphine complex, has been postulated to be the active catalyst in the synthesis of polygermanes by demethanative coupling of hydridogermanes.¹⁰ One impediment to rapid dehydrogenative catalytic turnover is the thermodynamic and kinetic stability of *fac*-(Me_3P)₃Ru(H)₃(SiR_3) complexes. The tridentate bis(imino)pyridine family of ligands seemed appropriate to enforce the desired *mer*-geometry and offered the advantage of convenient ligand tuning.² Furthermore, the known Ru(II) complex $[\text{N}_3^{\text{xy1}}]\text{RuCl}_2(\text{C}_2\text{H}_4)$ ¹¹ could serve as a convenient entry into the desired silyl and germyl complexes. Although a large number of tridentate pyridine ligand complexes of Ru(II), Ru(III), and Ru(IV) are known,^{2,3,5–7,11,12} there are very few reports of comparable Ru(0) complexes, and all of those involve strongly π -accepting co-ligands.¹³ Shiotsuki and co-workers isolated mononuclear ruthenium complexes containing terpy, 2,6-bis(imino)pyridine, and 2,6-bis(oxazolonyl)pyridine ligands as the bis(fumarates).¹³ Milstein and co-workers proposed the intermediacy of a $[\text{PNP}]\text{Ru}(0)$ complex ($[\text{PNP}] = \text{bis}(\text{phosphinomethyl})\text{-pyridine}$) in the catalytic dehydrogenation of alcohols to ketones. Although only Ru(II) complexes were isolated or directly observed in the catalytic reaction,^{14a} a related $[\text{PNP}]\text{Ru}(0)$ dicarbonyl derivative has been described very recently.^{14b} In this contribution we report the synthesis and characterization of five new formally $[\text{N}_3]\text{Ru}(0)$ complexes containing arene, dinitrogen, phosphine, and carbonyl ligands. The synthesis of silylene complexes from the reactions of $[\text{N}_3]\text{Ru}(0)$ complexes with hydrido- and chlorosilanes was

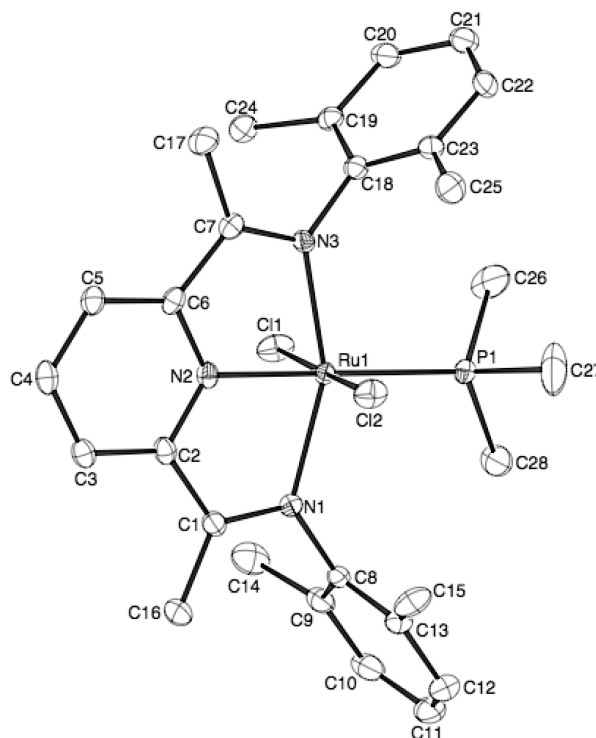


Figure 1. ORTEP drawing of $[\text{N}_3^{\text{xy1}}]\text{RuCl}_2(\text{PMe}_3)$ (30% thermal ellipsoids). Selected bond lengths (Å) and angles (deg): Ru1–N1, 2.116(3); Ru1–N2, 1.971(3); Ru1–N3, 2.121(2); Ru1–Cl1, 2.3567(10); Ru1–Cl2, 2.3902(10); Ru1–C12, 2.4016(10); N2–Ru1–P1, 179.68(9); N1–Ru1–N3, 155.15(10); Cl1–Ru1–Cl2, 177.54(4).

recently described in a preliminary communication from this group.¹⁵

Results

Phosphine and Carbonyl Complexes of $[\text{N}_3]\text{RuCl}_2$. Treatment of $[\text{N}_3^{\text{xy1}}]\text{RuCl}_2(\text{C}_2\text{H}_4)$ (**1a**) with PMe_3 or carbon monoxide at room temperature leads to ethylene loss and formation of the corresponding phosphine or carbonyl adducts *trans*- $[\text{N}_3^{\text{xy1}}]\text{RuCl}_2(\text{L})$ ($\text{L} = \text{PMe}_3, \text{CO}$), which can be isolated in 80–90% yields (eq 1). The $^31\text{P}\{^1\text{H}\}$ NMR of $[\text{N}_3^{\text{xy1}}]\text{RuCl}_2(\text{PMe}_3)$ exhibits one singlet at $\delta -5.77$ for the PMe_3 ligand. The CO ligand in $[\text{N}_3^{\text{xy1}}]\text{RuCl}_2(\text{CO})$ is observed as a singlet at $\delta 202.51$ in the $^{13}\text{C}\{^1\text{H}\}$ NMR spectrum. In the IR spectrum, the carbonyl complex exhibits ν_{CO} at 1963 cm^{-1} , only slightly higher than the value of 1948 cm^{-1} reported for $[(\text{mer}, \text{trans}-\text{RuCl}_2(\text{CO})(\text{NN}'\text{N}))]$ ($\text{NN}'\text{N} = 2, 6\text{-bis}[(\text{dimethylamino})\text{methyl}]\text{pyridine}$), which features saturated amines in the chelating ligand, rather the conjugated imines in the $[\text{N}_3]$ system.⁶

The solid-state structures of complexes *trans*- $[\text{N}_3^{\text{xy1}}]\text{RuCl}_2(\text{L})$ ($\text{L} = \text{PMe}_3, \text{CO}$) were determined by single-crystal X-ray diffraction methods. Both complexes exhibit a six-coordinate, pseudo-octahedral geometry with a *trans* arrangement of the two chloride ligands ($\text{L} = \text{PMe}_3$, Figure 1; $\text{L} = \text{CO}$, Figure 2). The main deviation from the ideal octahedral geometry is the *trans* $\text{N}_{\text{imine}}\text{-Ru-N}_{\text{imine}}$ bond angle ($\text{L} = \text{PMe}_3$, $155.15(10)^\circ$; $\text{L} = \text{CO}$, $153.58(8)^\circ$),

(8) Dioumaev, V. K.; Procopio, L. J.; Carroll, P. J.; Berry, D. H. *J. Am. Chem. Soc.* **2003**, *125*, 8043–8058.

(9) (a) Procopio, L. J.; Berry, D. H. *J. Am. Chem. Soc.* **1991**, *113*, 4039–4040. (b) Procopio, L. J.; Mayer, B.; Plössl, K.; Berry, D. H. *Polym. Prepr. Am. Chem. Soc., Div. Polym. Chem.* **1992**, *33*, 1241–1242. (c) Dioumaev, V. K.; Yoo, B. R.; Procopio, L. J.; Carroll, P. J.; Berry, D. H. *J. Am. Chem. Soc.* **2003**, *125*, 8936–8948. (d) Dioumaev, V. K.; Plössl, K.; Carroll, P. J.; Berry, D. H. *Organometallics* **2000**, *19*, 3374–3378. (e) Dioumaev, V. K.; Plössl, K.; Carroll, P. J.; Berry, D. H. *J. Am. Chem. Soc.* **1999**, *121*, 8391–8392.

(10) (a) Reichl, J. A.; Popoff, C. M.; Gallagher, L. A.; Remsen, E. E.; Berry, D. H. *J. Am. Chem. Soc.* **1996**, *118*, 9430–9431. (b) Katz, S. M.; Reichl, J. A.; Berry, D. H. *J. Am. Chem. Soc.* **1998**, *120*, 9844–9849. (c) Huo, Y.; Berry, D. H. *Chem. Mater.* **2004**, *17*, 157–163.

(11) Dias, E. L.; Brookhart, M.; White, P. S. *Organometallics* **2000**, *19*, 4995–5004.

(12) (a) del Rio, I.; Gossage, R. A.; Hannu, M. S.; Lutz, M.; Spek, A. L.; van Koten, G. *Organometallics* **1999**, *18*, 1097–1105. (b) Vogler, L. M.; Brewer, K. J. *Inorg. Chem.* **1996**, *35*, 818–824. (c) Chanda, N.; Sarkar, B.; Fiedler, J.; Kaim, W.; Lahiri, G. K. *J. Chem. Soc., Dalton Trans.* **2003**, 3550–3555. (d) Abbenhuis, R. A. T. M.; Boersma, J.; van Koten, G. *J. Org. Chem.* **1998**, *63*, 4282–4290. (e) del Rio, I.; van Koten, G. *Organometallics* **2000**, *19*, 361–364. (f) Welch, T. W.; Cifan, S. A.; White, P. S.; Thorp, H. H. *Inorg. Chem.* **1997**, *36*, 4812–4821. (g) Meyer, T. J.; Huynh, M. H. V. *Inorg. Chem.* **2003**, *42*, 8140–8160.

(13) Shiotsuki, M.; Suzuki, T.; Iida, K.; Ura, Y.; Wada, K.; Kondo, T.; Mitsudo, T. *Organometallics* **2003**, *22*, 1332–1339.

(14) (a) Zhang, J.; Gandelman, M.; Shimon, L. J.; Rozenberg, H.; Milstein, D. *Organometallics* **2004**, *23*, 4026–4033. (b) Salem, H.; Shimon, L. J. W.; Diskin-Posner, Y.; Leitun, G.; Ben-David, Y.; Milstein, D. *Organometallics* **2009**, *28*, 4971–4806.

(15) Yoo, H.; Carroll, P. J.; Berry, D. H. *J. Am. Chem. Soc.* **2006**, *128*, 6038–6039.

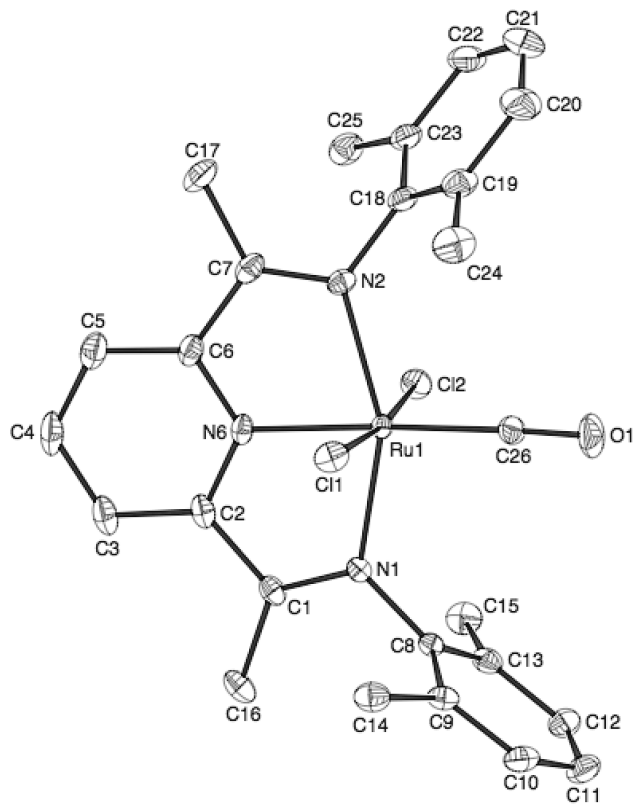
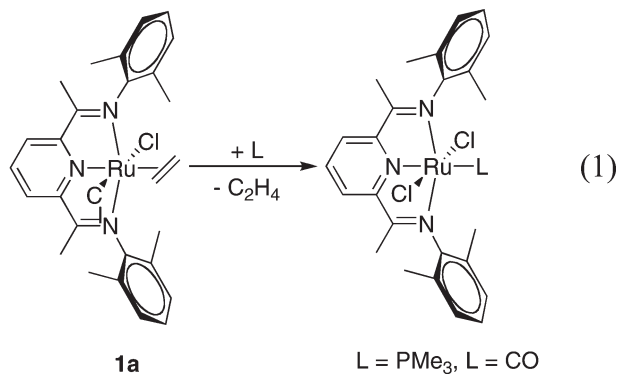


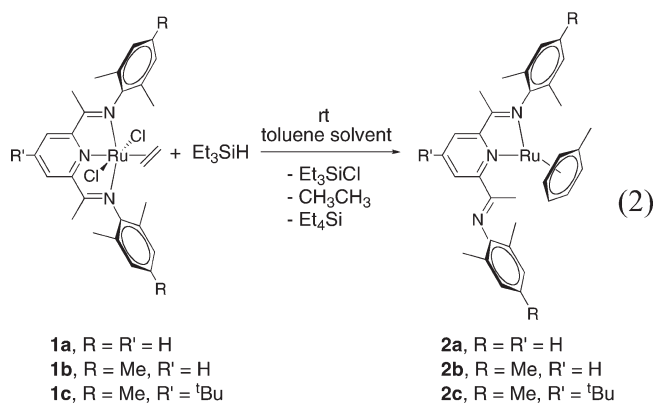
Figure 2. ORTEP drawing of $[\text{N}_3^{\text{xylyl}}]\text{RuCl}_2(\text{CO})$ (30% thermal ellipsoids). Selected bond lengths (\AA) and angles (deg): Ru1–N1, 2.108(2); Ru1–N2, 2.130(2); Ru1–N6, 2.0056(19); Ru1–C26, 1.870(3); Ru1–Cl1, 2.4045(7); Ru1–Cl2, 2.3930(7); C26–O1, 1.149(3); N6–Ru1–C26, 177.11(10); N1–Ru1–N2, 154.68(8); Cl1–Ru1–Cl2, 173.15(2). Chlorobenzene solvent of crystallization omitted.

which is typical for bis(imino)pyridyl complexes.^{2,11} The xylyl groups are oriented approximately perpendicular to the $[\text{N}_3]$ ligand plane. Although only the *trans* isomers of $[\text{N}_3^{\text{xylyl}}]\text{RuCl}_2(\text{L})$ are observed, both *cis* and *trans* isomers have been previously reported for the triphenylphosphine and carbonyl adducts of related ruthenium complexes.^{2,6,16}



Reduction of $[\text{N}_3]\text{RuCl}_2(\text{C}_2\text{H}_4)$ with R_3SiH : Synthesis of Ru(0) Arene Complexes. Treatment of the $[\text{N}_3]\text{Ru}(\text{II})$ ethylene adducts **1a,b,c** ($[\text{N}_3^{\text{xylyl}}] = 2,6\text{-(Xyl)NCMe}_2\text{C}_5\text{H}_3\text{N}$, **1a**; $[\text{N}_3^{\text{mes}}] = 2,6\text{-(Mes)NCMe}_2\text{C}_5\text{H}_2\text{N}$, **1b**; $[\text{N}_3^{\text{mes}}] = 2,6\text{-(Mes)NCMe}_2\text{p-}^t\text{BuC}_5\text{H}_2\text{N}$, **1c**) with excess Et_3SiH

(or Me_3SiH) in an arene solvent (e.g., toluene or benzene) leads to formation of intensely purple $[\kappa^2\text{-N}_3]\text{Ru}(\eta^6\text{-arene})$ complexes (**2a,b,c**) isolated in 75–85% yield (eq 2). GC and ^1H NMR analysis indicates the concurrent production of Et_3SiCl , Et_4Si , and ethane. An intermediate ruthenium hydride complex can be observed by ^1H NMR during the reduction of **1a** and is tentatively assigned as $[\text{N}_3^{\text{xylyl}}]\text{Ru}(\text{H})(\text{Cl})(\text{C}_2\text{H}_4)$ on the basis of an upfield resonance for the Ru–H characteristic of a *trans* Cl–Ru–H arrangement ($\delta -21.91$, 1H) and a resonance for coordinated ethylene ($\delta 4.12$, 4H) that is fluxional on the NMR time scale. The PMe_3 complex $[\text{N}_3^{\text{xylyl}}]\text{RuCl}_2(\text{PMe}_3)$ does not react with silanes at room temperature, but leads to $[\text{N}_3^{\text{xylyl}}]\text{Ru}(\text{H})(\text{Cl})(\text{PMe}_3)$ after 3.5 h at 150 °C. The Ru–H resonance for the phosphine complex is observed as a doublet at $\delta -19.17$ ($^2J_{\text{P-H}} = 42.5$ Hz) in the ^1H NMR, similar to the intermediate in the reduction of **1a**. Further heating of $[\text{N}_3^{\text{xylyl}}]\text{RuCl}_2(\text{PMe}_3)$ with silanes leads to extensive decomposition.



Arene complexes **2** exhibit “two-legged piano-stool” geometries, with a bidentate $[\text{N}_3]$ ligand necessary to maintain the $18e^-$ count at ruthenium and provide steric relief at the metal center. This “arm-off” coordination mode leads to chemically inequivalent xylyl (or mesityl) and imine methyl groups in the NMR spectra. The coordinated arene ligand in **2** is labile and undergoes exchange with other arenes within minutes at room temperature. The structure of **2a** was confirmed by crystallography (Figure 3). Bidentate (κ^2) coordination of potentially tridentate $[\text{N}_3]$ ligands has been previously observed in low-valent complexes of several metals.^{4c,17}

Synthesis and Structure of Ru(0) μ -Dinitrogen Complexes. Treatment of the $[\kappa^2\text{-N}_3]\text{Ru}(\eta^6\text{-arene})$ complexes with dinitrogen in non-arene solvents at room temperature leads to a color change from dark purple to intense turquoise and formation of equilibrium mixtures containing **2** and Ru(0) bridging dinitrogen complexes, **3** (eq 3). In the case of xylyl-substituted **2a**, the slightly higher solubility of the starting complexes in hexanes can be exploited, and **3a** can be prepared in 80–90% yield by stirring a slurry of **2a** under N_2 for 2 days. The bridging dinitrogen ligand is labile, and **3** rapidly reverts to **2** in arene solvents. It should be noted that the dinitrogen complexes are pyrophoric solids and burst into flames

(16) Ben-Hadda, T.; Mountassir, C.; Le Bozec, H. *Polyhedron* **1995**, *14*, 953–955.

(17) (a) Shirin, Z.; Mukherjee, R.; Richardson, J. F.; Buchanan, R. M. *J. Chem. Soc., Dalton Trans.* **1994**, 465–469. (b) Lu, S.; Selbin, J. *Inorg. Chim. Acta* **1987**, *134*, 229–232. (c) Albon, J. M.; Edwards, D. A.; Moore, P. J. *Inorg. Chim. Acta* **1989**, *159*, 19–22.

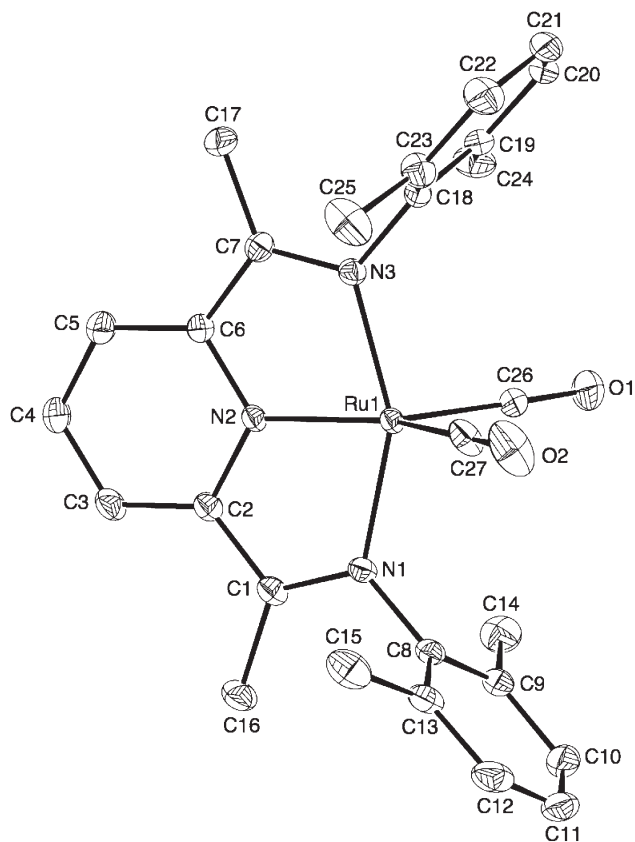
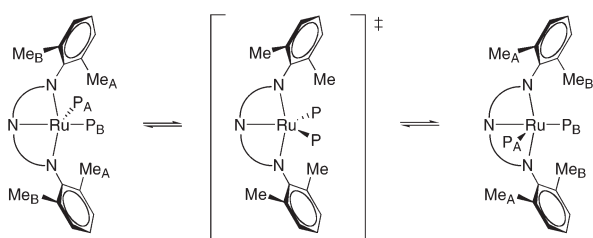


Figure 6. ORTEP drawing of $[\text{N}_3^{\text{xy}1}]\text{Ru}(\text{CO})_2$, **6a** (30% thermal ellipsoids). Selected bond lengths (Å) and angles (deg): Ru1–N1, 2.072(2); Ru1–N2, 1.947(2); Ru1–N3, 2.062(2); Ru1–C26, 1.878(3); Ru1–C27, 1.884(3); C26–O1, 1.144(3); C27–O2, 1.146(3); N3–Ru1–N1, 153.58(8); N2–Ru1–C26, 130.60(10); N2–Ru1–C27, 140.74(11); C26–Ru1–C27, 88.65(12).

Scheme 1. Intramolecular Exchange of Phosphines in Compound 5a

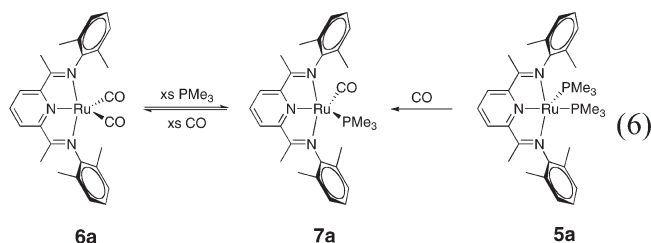


phosphine ligand environments and, thus, does not require rotation around the N–xylyl bonds. Intramolecular phosphine exchange presumably occurs via a symmetrical TBP geometry, which is the observed ground state for the analogous dicarbonyl complex (vide infra).

Dicarbonyl complex **6a** was isolated in 78% yield as a green solid following treatment of **2a** with carbon monoxide (room temperature, 1 atm). Strong bands for the terminal carbonyl ligands ($\nu_{\text{CO}} = 1925$ and 1778 cm^{-1}) are observed in the IR spectrum of **6a**. The structure of dicarbonyl complex **6a** as determined in the solid state is shown in Figure 6. Although the geometry is best described as trigonal bipyramidal with both CO ligands in the equatorial plane, the OC–Ru–CO angle is quite small ($88.66(12)^\circ$) and the two $\text{N}_{\text{pyr}}\text{–Ru–CO}$ angles differ by ca. 10° ($130.60(10)^\circ$ and

$140.76(11)^\circ$). In other words, the $\text{Ru}(\text{CO})_2$ fragment is slightly (5°) canted toward the square-pyramidal geometry exhibited by **5a**. The ruthenium center lies slightly above the plane ($0.074(1) \text{ \AA}$) of the $[\text{N}_3]$ ligand, but much less so than in the bis(phosphine) complex, **5a**.

Reaction of **6a** with excess PMe_3 at 25°C leads to the formation of $[\text{N}_3^{\text{xy}1}]\text{Ru}(\text{PMe}_3)(\text{CO})$, **7a**, isolated as an orange solid in 72% yield (eq 6). Similarly, treatment of **5a** with CO also generates **7a**, but this path is less useful synthetically, as the reaction proceeds readily to produce **6a**. The $^{31}\text{P}\{^1\text{H}\}$ NMR spectrum of **7a** exhibits one singlet at δ 1.54 for the PMe_3 ligand, and the CO ligand is observed as a doublet at δ 206.12 ($^2J_{\text{PC}} = 27.7 \text{ Hz}$) in the $^{13}\text{C}\{^1\text{H}\}$ NMR spectrum. Complex **7a** exhibits ν_{CO} at 1865 cm^{-1} in the IR spectrum, consistent with a monocarbonyl Ru(0) species. In comparison, the carbonyl stretch in the Ru(II) monocarbonyl complex $[\text{N}_3^{\text{xy}1}]\text{RuCl}_2(\text{CO})$ is found at much higher energy (1963 cm^{-1} , vide supra). It is interesting that the bis(phosphine) complex reacts readily with CO, but does not undergo intermolecular exchange with $\text{PMe}_3\text{-}d_9$, suggesting substitution does not occur by initial dissociation of phosphine from **5a**, but rather by a sterically sensitive associative path. The most likely possibility would involve dissociation of an imine arm of the chelate (cf. compound **2**), although associative attack of CO on the $18e^-$ **5a** cannot be excluded at this time.



Complex **7a** has also been characterized by X-ray diffraction methods (Figure 7). The geometry of **7a** can best be described as situated between square pyramidal (SP) and trigonal bipyramidal (TBP), with the CO ligand lying in the apical position ($\text{N2–Ru1–C26} = 117.59(15)^\circ$; $\text{C26–Ru1–P1} = 85.24(13)^\circ$), pseudo-*trans* to the vacant coordination site. The ruthenium center is displaced by $0.262(3) \text{ \AA}$ toward the carbonyl ligand from the plane formed by the $[\text{N}_3]$ ligand, or about half the displacement in the bis(phosphine) **5a** ($0.469(1) \text{ \AA}$).

The vast majority of five-coordinate d^6 , Ru(II) complexes exhibit a square-pyramidal geometry, except for sterically hindered complexes that require the less congested TBP environment.²⁴ On the other hand, most five-coordinate d^8 , Ru(0) complexes containing carbonyl ligands prefer a TBP ground-state geometry.^{25,26} The preference for equatorial binding by π -acceptor ligands predicted by Hoffman appears to be a contributing factor.²⁵ Comparison of the five-coordinate complexes **5–7** reveals a consistent progression from square pyramidal to trigonal pyramidal with the

(24) (a) Huang, D.; Streib, W. E.; Bollinger, J. C.; Caulton, K. G.; Winter, R. F.; Scheiring, T. *J. Am. Chem. Soc.* **1999**, *121*, 8087–8097. (b) Crochet, P.; Gimeno, J.; Garc a-Granda, S.; Borge, J. *Organometallics* **2001**, *20*, 4369–4377. (c) MacFarlane, K. S.; Joshi, A. M.; Rettig, S. J.; James, B. R. *Inorg. Chem.* **1996**, *35*, 7304–7310. (d) Heyn, R. H.; Huffman, J. C.; Caulton, K. G. *New J. Chem.* **1993**, *17*, 797–803.

(25) (a) Rossi, A. R.; Hoffmann, R. *Inorg. Chem.* **1975**, *14*, 365–374. (b) Elian, M.; Hoffmann, R. *Inorg. Chem.* **1975**, *14*, 1058–1076.

(26) Muetterties, E. L. *Acc. Chem. Res.* **1970**, *3*, 266–273.

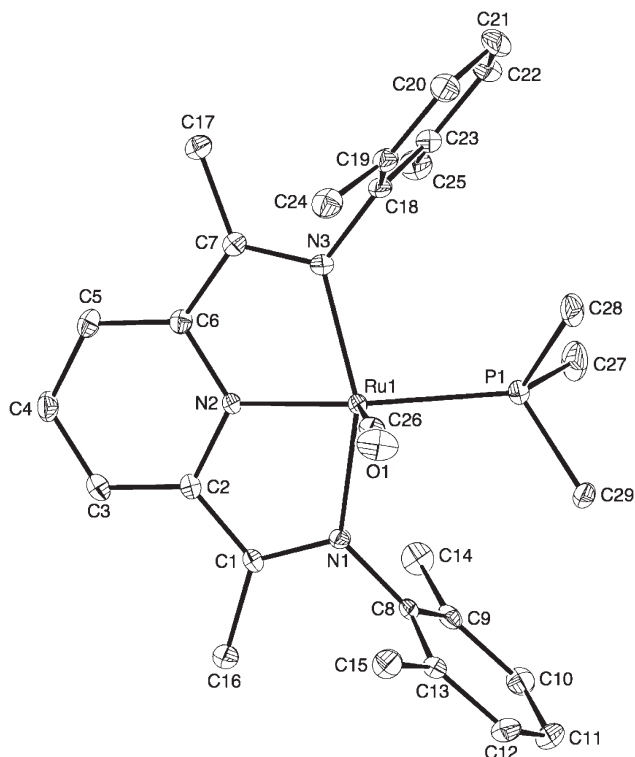


Figure 7. ORTEP drawing of $[N_3^{xy1}]Ru(PMe_3)(CO)$, **7a** (30% thermal ellipsoids). Selected bond lengths (Å) and angles (deg): Ru1–N1, 2.094(3); Ru1–N2, 1.964(3); Ru1–N3, 2.088(3); Ru1–C26, 1.835(4); Ru1–P1, 2.3446(11); C26–O1, 1.165(5); N3–Ru1–N1, 150.47(12); N2–Ru1–C26, 117.59(16); N2–Ru1–P1, 157.17(9); C26–Ru1–P1, 85.24(13).

introduction of smaller, π -acceptor CO ligands. The degree of displacement of the metal from the $[N_3]$ ligand plane also changes with the nature of the co-ligands: **5a** (0.469(1) Å) > **7a** (0.262(3) Å) > **6a** (0.074(1) Å). Virtually identical trends are seen in the structurally characterized Ru(0) complexes, $(dmpe)_2Ru(L)$ ($L = PMe_3, CO$), in which the phosphine derivative adopts a SP geometry with the ruthenium above the ligand square plane (0.53 Å), and the carbonyl adduct exhibits a TBP geometry.^{27d} Caulton, Eisenstein, and co-workers recently reported theoretical calculations of steric and electronic effects in the model complex $Ru(CO)_2(PH_3)_3$, revealing a very small (< 5 kcal/mol) electronic preference for carbonyl ligands in the equatorial position, and thus steric factors can easily dictate the geometry.^{28,37} Steric factors may well determine the apical—not equatorial—position of the CO ligand in the solid-state structure of **7a**.

Treatment of either of the $[N_3^{xy1}]Ru(0)$ complexes **2** or **3** with ethylene leads to rapid formation of the $[N_3^{xy1}]RuL_2$ complex **4a** ($L_{1,2} = C_2H_4$). Unlike the phosphine and

carbonyl derivatives, the bis(ethylene) complex **4a** is labile and is stable only in solution under an ethylene atmosphere. Complex **4a** has not been isolated as a pure solid, but displays three singlets at δ 2.28 (6H), 1.76 (12H), and 1.63 (8H) in the 1H NMR spectrum, assigned as the chemically equivalent imine methyl groups, xylyl methyl groups, and two ethylene ligands respectively. The 1H NMR data are consistent with a symmetrical trigonal-bipyramidal geometry in which the ethylene protons are averaged by rapid rotation or dissociation. A comparable geometry was previously observed for the bis(dimethyl fumarate) pyridine complexes reported by Mitsudo and co-workers, although the olefin ligands are not dynamic on the NMR time scale in those complexes.¹³

Discussion

Stability and Scope of Reactivity of the Ruthenium(0) Complexes. The chemical reduction of **1a** provides convenient access to **2–7**, all of which are formally Ru(0), d^8 complexes. Other than mononuclear and cluster carbonyl complexes,²⁹ there are relatively few examples of isolated Ru(0) species.^{15,27,30} Triethylsilane is an excellent reducing agent for **1**, as it is sufficiently mild to avoid over-reduction or deprotonation,^{4c,31} and also provides for the irreversible removal of ethylene by hydrogenation or hydrosilylation. Furthermore, only volatile byproducts are generated, which simplifies workup.

The η^6 -arene complexes **2** are the easiest to prepare and serve as versatile starting materials for subsequent reactions. It is interesting to note that **1** is produced by displacing an arene from $[(p\text{-cymene})RuCl_2]_2$, but that reduction of **1** to **2** favors coordination of arene at the expense of coordination of one of the chelate arms. This “arm on/arm off” phenomenon has been observed for bis(imino)pyridyl complexes of Mo and $W^{17b,c}$ and for related tridentate ligands with ruthenium.^{17a} Recently, Chirik and co-workers reported an intramolecular version of the equilibrium in eq 3 for an iron complex, in which a coordinated imine nitrogen dissociates to permit intramolecular η^6 coordination of an arene substituent on the imine nitrogen.^{4c} The facile arene exchange in **2** and equilibrium reaction to form the tridentate **3** highlights the lability of the arene and versatility of the bis(imino)-pyridyl ligand.

The bridging dinitrogen complex **3** is of interest for several reasons. The first example of a bridging N_2 ligand was the diruthenium complex prepared by the Taube group in 1968³²

(27) (a) McKinney, R. J.; Colton, M. C. *Organometallics* **1986**, *5*, 1080–1085. (b) Al-Ohalay, A.; Head, R. A.; Nixon, J. F. *J. Organomet. Chem.* **1981**, *205*, 99–110. (c) Pertici, P.; Vitulli, G.; Paci, M.; Porri, L. *J. Chem. Soc., Dalton Trans.* **1980**, 1961–1964. (d) Jones, W. D.; Libertini, E. *Inorg. Chem.* **1986**, *25*, 1794–1800. (e) Flügel, R.; Windmüller, B.; Gevert, O.; Werner, H. *Chem. Ber.* **1996**, *129*, 1007–1013. (f) Ogasawara, M.; Macgregor, S. A.; Streib, W. E.; Folting, K.; Eisenstein, O.; Caulton, K. G. *J. Am. Chem. Soc.* **1995**, *117*, 8869–8870. (g) Huang, D.; Streib, W. E.; Eisenstein, O.; Caulton, K. G. *Organometallics* **2000**, *19*, 1967–1972.

(28) (a) Kaupp, M.; von Schnering, H. G. *Angew. Chem., Int. Ed. Engl.* **1995**, *34*, 986. (b) Snyder, J. P. *Angew. Chem., Int. Ed. Engl.* **1995**, *34*, 986–987. (c) Ward, M. D.; McCleverty, J. A. *J. Chem. Soc., Dalton Trans.* **2002**, 275–288. (d) Pierpont, C. G. *Coord. Chem. Rev.* **2001**, *216*, 99–125.

(29) (a) Whittlesey, M. K. In *Comprehensive Organometallic Chemistry III*; Mingos, D. P. M., Crabtree, R. H., Eds.; Elsevier: Amsterdam, 2007. (b) Bruce, M. I.; Stone, F. G. A. *Angew. Chem., Int. Ed. Engl.* **1968**, *7*, 427–432. (c) Sappa, E. *J. Cluster Sci.* **1994**, *5*, 211–263.

(30) (a) Suzuki, T.; Shiotsuki, M.; Wada, K.; Kondo, T.; Mitsudo, T. *Organometallics* **1999**, *18*, 3671–3678. (b) Suzuki, T.; Shiotsuki, M.; Wada, K.; Kondo, T.; Mitsudo, T. *J. Chem. Soc., Dalton Trans.* **1999**, 4231–4237. (c) Shiotsuki, M.; Suzuki, T.; Kondo, T.; Wada, K.; Mitsudo, T. *Organometallics* **2000**, *19*, 5733–5743. (d) Shiotsuki, M.; Miyai, H.; Ura, Y.; Suzuki, T.; Kondo, T.; Mitsudo, T. *Organometallics* **2002**, *21*, 4960–4964. (e) Ura, Y.; Sato, Y.; Shiotsuki, M.; Suzuki, T.; Wada, K.; Kondo, T.; Mitsudo, T. *Organometallics* **2003**, *22*, 77–82.

(31) (a) Sugiyama, H.; Ghazar, A.; Gambarotta, S.; Yap, G. P. A.; Budzelaar, P. H. M. *J. Am. Chem. Soc.* **2002**, *124*, 12268–12274. (b) Khorobkov, I.; Gambarotta, S.; Yap, G. P. A.; Budzelaar, P. H. M. *Organometallics* **2002**, *21*, 3088–3090. (c) Enright, D.; Gambarotta, S.; Yap, G. P. A.; Budzelaar, P. H. M. *Angew. Chem., Int. Ed.* **2002**, *41*, 3873–3876. (d) Bouwkamp, M. W.; Lobkovsky, E.; Chirik, P. J. *Inorg. Chem.* **2006**, *45*, 2–4.

(32) Harrison, D. F.; Weissberger, E.; Taube, H. *Science* **1968**, *159*, 320–322.

and structurally characterized by Gray and co-workers in 1969.^{18c} Although many similar complexes have been subsequently isolated, all involve unambiguously d^6 , Ru(II) centers and typically with octahedral geometries.^{6,9e,18} The $16e^-$ Ru(0) dinitrogen complex **3** exhibits a square-planar geometry in the solid state, mostly likely due to steric factors that disfavor coordination of an additional terminal nitrogen ligand in the apical position, although reversible binding of additional nitrogen ligands in solution has not been excluded. The bulky aryl rings on each half of the complex effectively encapsulate the metal centers and bridging nitrogen ligand, which also contributes to the stability of this reduced species. Until quite recently, non-macrocyclic, four-coordinate ruthenium complexes were relatively rare. Tetrahedral geometry is most typical,³³ but Wilkinson reported a square-planar bis(imido) ruthenium complex in 1992, and Caulton, Werner, and others have isolated several square-planar ruthenium complexes, including a $14e^-$ (amido)-(bisphosphine) complex that exhibits a high-spin ground state.^{27c,g,34} The paucity of square-planar Ru(0) complexes is somewhat surprising, as isoelectronic $16e^-$, d^8 Rh(I) and Pt(II) species are extremely common. However, such species have been proposed as reaction intermediates or generated as a short-lived transient species through flash photolysis and matrix isolation.^{14,35}

It is worth noting the relative advantages and disadvantages of **2** and **3** as starting materials for subsequent reactions. The arene complexes are generally easier to synthesize and purify, are more soluble in nonpolar solvents than the dinitrogen complexes, and are stable in arene solvents (although one must be mindful of the facile arene exchange). However, an inherent disadvantage of the arene complexes is that most reactions liberate the arene ligand (toluene, benzene), and this byproduct can complicate the workup of reactions that remain in equilibrium with the starting complex. On the other hand, the pyrophoric dinitrogen complex **3** is prepared from arene complex **2**, which introduces an additional synthetic step and precludes use of arene solvents in subsequent reactions. Compound **3** is also less stable than the arene complexes, decomposing above 60 °C in solution, whereas **2** is stable for hours at 95 °C. However, **3** is more reactive than **2**, exhibits shorter reaction times, and produces only gaseous nitrogen as a byproduct.

Ligand Non-innocence in $[N_3]Ru$ Complexes and Formal Oxidation States. Electronic structure and the nature of the bonding in metal/ligand complexes are fundamental issues in

inorganic and organometallic chemistry.^{36,37,28,38} The ambiguity of formal oxidation states—particularly in complexes containing ligands capable of accepting metal electron density via π -back-bonding—has long been recognized. Recently, increased attention has been devoted to understanding the “non-innocent” character of some ligand classes in somewhat different terms. In certain cases, $[N_3^A]M$ complexes may be best described by forms representing full transfer of one or more electrons to relatively remote orbitals on the ligand. Several groups have shown that surprisingly complex electronic structures and magnetic behavior can result in these *formally* low-valent complexes.^{22,23,38a,39}

In extreme cases, such as in some metal catecholate/semi-quinonate complexes, equilibria can be observed between separate valence tautomers in which an unpaired electron can be localized on either the metal or the ligand.^{28c,d,36,40} For example, Kaim and co-workers investigated ruthenium complexes of “non-innocent” ligands^{12c} such as *o*-iminoquinone or *o*-iminothioquinone and documented “redox isomerism” (valence tautomerism)^{28d} that effectively allows variation of *formal* oxidation states from Ru(II) to Ru(IV).³⁶ On the basis of structural and EPR studies it was concluded that most members of that particular series are best described as Ru(III).

Similarly, the Ru(0)/Ru(II) continuum has been probed by Caulton, Eisenstein, and co-workers as part of an extensive series of papers on low-coordinate and low-valent ruthenium complexes. These ruthenium phosphine nitrosyl complexes can accommodate Ru(0) and Ru(II) oxidation states through tautomerization of the NO ligand.^{27e,g,37}

More commonly, π -back-bonding is not sufficient to warrant a change in oxidation state formalism, but rather involves the more subtle issue of relative “electron richness” at the metal center. For example, the metal centers in both $W(CO)_6$ and $W(PMe_3)_6$ are both assigned an unambiguous *formal* oxidation state of W(0), yet there would be little disagreement that the carbonyl ligands delocalize substantial electron density away from the metal center in the former and that the tungsten in the latter is more “electron rich”. More importantly, the latter behaves in chemical reactions as a highly reduced species, whereas the reactivity of $W(CO)_6$ is more temperate.

Given the potential “non-innocent” character of bis(imino)pyridyl ligands, the question arises as to the best electronic description of complexes **2** and **3**. The bis(imino)pyridine in four-coordinate **3** would be classified using common conventions as a neutral donor ligand, and the metal as formally zerovalent, although even novice practitioners would note the possibility for substantial electron delocalization into the ligand to reduce electron density at Ru. Taking into account ligand non-innocence by explicitly specifying metal-to-ligand electron transfer results in

(33) (a) Sánchez-Delgado, R. A.; Navarro, M.; Lazardi, K.; Atencio, R.; Capparelli, M.; Vargas, F.; Urbina, J. A.; Bouillez, A.; Noels, A. F.; Masi, D. *Inorg. Chim. Acta* **1998**, *275–276*, 528–540. (b) Hay-Motherwell, R. S.; Wilkinson, G.; Hussain-Bates, B.; Hursthouse, M. B. *J. Chem. Soc., Dalton Trans.* **1992**, 3477–3482. (c) Savage, P. D.; Wilkinson, G.; Motevalli, M.; Hursthouse, M. B. *J. Chem. Soc., Dalton Trans.* **1988**, 669–673. (d) Gaughan, A. P., Jr.; Corden, B. J.; Eisenberg, R.; Ibers, J. A. *Inorg. Chem.* **1974**, *13*, 786–791.

(34) (a) Danopoulos, A. A.; Wilkinson, G.; Hussain-Bates, B.; Hursthouse, M. B. *Polyhedron* **1992**, *11*, 2961–2964. (b) Watson, L. A.; Ozerov, O. V.; Pink, M.; Caulton, K. G. *J. Am. Chem. Soc.* **2003**, *125*, 8426–8427. (c) Yamamoto, Y.; Satoh, R.; Tanase, T. *J. Chem. Soc., Dalton Trans.* **1995**, 307–311.

(35) (a) Cole-Hamilton, D. J.; Wilkinson, G. *J. Am. Chem. Soc.* **1978**, 883–884. (b) Chatt, J.; Davidson, J. M. *J. Chem. Soc.* **1965**, 843–855. (c) Mawby, R. J.; Perutz, R. N.; Whittlesey, M. K. *Organometallics* **1995**, *14*, 3268–3274. (d) Hall, C.; Jones, W. D.; Mawby, R. J.; Osman, R.; Perutz, R. N.; Whittlesey, M. K. *J. Am. Chem. Soc.* **1992**, *114*, 7425–7435. (e) Bogdan, P. L.; Weitz, E. *J. Am. Chem. Soc.* **1989**, *111*, 3163–3167.

(36) Patra, S.; Sarkar, B.; Mobin, S. M.; Kaim, W.; Lahiri, G. K. *Inorg. Chem.* **2003**, *42*, 6469–6473.

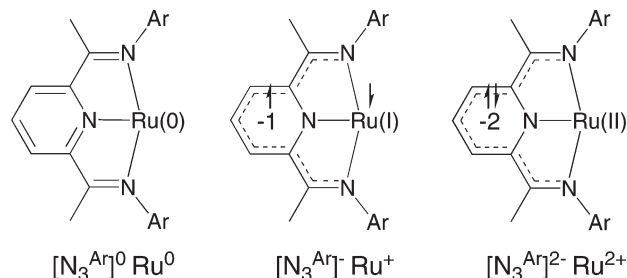
(37) Ogasawara, M.; Huang, D.; Streib, W. E.; Huffman, J. C.; Gallego-Planas, N.; Maseras, F.; Eisenstein, O.; Caulton, K. G. *J. Am. Chem. Soc.* **1997**, *119*, 8642–8651.

(38) (a) Vidyaratne, I.; Gambarotta, S.; Korobkov, I.; Budzelaar, P. H. M. *Inorg. Chem.* **2005**, *44*, 1187–1189. (b) Vidyaratne, I.; Scott, J.; Gambarotta, S.; Korobkov, I.; Budzelaar, P. H. M. *Inorg. Chem.* **2007**, *46*, 7040–7049. (c) Knijnenburg, Q.; Gambarotta, S.; Budzelaar, P. H. M. *Dalton Trans.* **2006**, 5442–5448.

(39) Sugiyama, H.; Korobkov, I.; Gambarotta, S.; Möller, A.; Budzelaar, P. H. M. *Inorg. Chem.* **2004**, *43*, 5771–5779.

(40) Da Silva, R. S.; Gorelsky, S. I.; Dodsworth, E. S.; Tfouni, E.; Lever, A. B. P. *J. Chem. Soc., Dalton Trans.* **2000**, 4078–4088.

Scheme 2. Diamagnetic Electron Transfer Valence Tautomers Involving Low-Spin Ruthenium



potential formalisms ranging from Ru(0) with a neutral ligand, to Ru(I) with a radical anion ligand, to Ru(II) with a dianionic ligand (Scheme 2). The matter of magnetic properties is further complicated by the possibility of low- or high-spin states on the metal, the small singlet/triplet separation of the $[N_3]^{2-}$ dianion,²² and the potential for spin coupling between unpaired electrons on the metal and ligand. For example, some of Chirik's $[N_3]Fe(L)$ complexes exhibit overall $S = 1$ and are conventionally depicted as neutral $[N_3]$ ligand/Fe(0) (d^8), but are more accurately described as triplet $[N_3]^{2-}$ /high-spin Fe(II) (d^6), with two unpaired electrons on the ligand and four unpaired electrons of opposite spin on the iron!²² In the present case, ruthenium nitrogen complex **3** is diamagnetic, and invoking the analogous triplet ligand dianion coupled to an $S = 1$, d^6 second-row metal center seems unnecessarily convoluted in the absence of any experimental evidence. Thus only formalisms involving low-spin ruthenium are considered in Scheme 2.

The question of whether an alternative representation (e.g., $[N_3]^{2-}/Ru(II)$) is more "accurate" is nontrivial and can require nonroutine computational studies such as "broken symmetry" methods. However, the value of formal oxidation states and d-electron counts lies in their utility, and the question of which formal representation is most "useful" or "descriptive" can be partially addressed by examining the spectroscopic data and structural parameters of the "Ru(0)" and "Ru(II)" complexes.

The dicarbonyl complex **6a** exhibits two CO stretches at 1925 and 1978 cm^{-1} . Ru(0) dicarbonyl complexes containing donor co-ligands that are not significant π -acceptors such as $Ru(CO)_2L_3$ ($L = PMePh_2$, PEt_3 , and $[P(2-furyl)_3]$) display two CO stretching bands in the ranges 1827–1844 and 1883–1900 cm^{-1} , about 90 cm^{-1} lower energy than in **6a**.⁴¹ On the other hand, CO vibrations in Ru(II) complexes such as $L_2RuCl_2(CO)_2$ ($L = PMe_3$ or PPh_3) (1985–1996 and 2049–2058 cm^{-1}) are about 60–70 cm^{-1} higher than in **6a**.⁴² Thus this traditional measure suggests the electron density at the metal is intermediate between that in less ambiguous examples of the Ru(0) and Ru(II) formalisms.

The carbonyl stretching energies in **6a** are quite similar to those in an analogous Fe(0) dicarbonyl complex, $[N_3^{iPr}]Fe(CO)_2$ (1914 and 1974 cm^{-1}), recently reported by Chirik and co-workers.^{4a} Interestingly, although broken symmetry DFT calculations suggest the $[N_3]^{2-}/Fe(II)$ formalism is most appropriate for a variety of other reduced

$[N_3^{iPr}]Fe$ complexes,²² the authors comment that both calculations and Mossbauer spectroscopy are consistent with the neutral ligand/Fe(0) formulation for $[N_3^{iPr}]Fe(CO)_2$. Again, the IR data for both the iron and ruthenium complexes are easily accommodated by the traditional M(0) oxidation state, combined with moderate competition for π -electron density between carbonyl and $[N_3]$ ligands.

A similar picture emerges for the monocarbonyl complex **7a**, which exhibits a CO stretch (1865 cm^{-1}) somewhat higher in energy than that of $(dmpe)_2Ru(CO)$ (1845 cm^{-1} , Ru(0)),^{27d,35d} but significantly lower than Ru(II) monocarbonyl complexes devoid of other π -acceptors, such as $(P^iPr_3)_2RuX_2(CO)$ ($X = Cl, H, I$; 1910–1920 cm^{-1}).⁴³ The IR spectrum of the formally Ru(II) complex $[N_3^{xyl}]RuCl_2(CO)$ is also consistent with some delocalization of electron density from Ru to the $[N_3]$ ligand, as the CO stretch (1963 cm^{-1}) is about 50 cm^{-1} higher energy than in $(P^iPr_3)_2RuX_2(CO)$.

In the absence of isotopic labeling studies and Raman data, the assignment of a weak band at 1856 cm^{-1} in the IR spectrum of dinitrogen complex **3a** as the N–N stretch must be viewed as tentative, but does suggest a rather electron-rich metal center. Although much lower than reported for μ -dinitrogen complexes containing unambiguously Ru(II) centers (2000–2150 cm^{-1}),^{5,9e,18} this value for the N–N stretch is not extraordinary compared with recent reports of low-valent Fe–Fe systems such as $(LFe)_2(\mu-N_2)$ ($L =$ bulky β -diketiminate ligand),⁴⁴ which exhibits ν_{NN} at 1778 cm^{-1} (Raman), an extremely long N–N triple-bond distance (1.182(5) Å), and short Fe–N₂ distances (1.77–1.78(5) Å). Thus, the low N–N stretch (1856 cm^{-1}) in **3a** and the elongated N–N bond length (1.161(5) Å) in **3c** are internally consistent and indicate greater reduction of the N–N bond order—and hence greater "low-valent" character—than in typical Ru(II) nitrogen complexes. Somewhat in contrast, Gambarotta and co-workers have made a strong case for the dianionic formalism for the bis(imino)pyridine ligand in the case of a vanadium bridging dinitrogen complex, $\{[N_3^{iPr}]V(THF)\}_2(\mu-N_2)$.^{38a} The bridging dinitrogen ligand in this early metal complex is apparently highly reduced ($D(NN) = 1.259(6)$ Å) and can be viewed as a dianion. On the basis of bond lengths within the $[N_3]$ ligand and DFT calculations, these workers interpret the paramagnetism of the complex as resulting from two noninteracting high-spin V(III) centers, each with a $[N_3]$ ligand dianion and bridged by a N_2^{2-} ligand. In this context, the ruthenium centers in **3b** are clearly less electron releasing toward the dinitrogen than the $[N_3]V$ centers.

The degree of electron delocalization—whether best described as π -back-bonding or complete electron transfer to the $[N_3]$ ligand—is also reflected in the intraligand bond distances. The $C=N_{im}$ and $C_{pyr}-C_{im}$ distances in bis(imino)pyridine ligands have been described as particularly diagnostic of the degree of electron transfer from the central metal,^{38c} with longer $C=N$ and shorter $C_{pyr}-C_{im}$ bonds associated with the $[N_3]$ and $[N_3]^{2-}$ formulations. It must be noted, however, that traditional " π -back-bonding" predicts exactly the same trends. Gambarotta has suggested rough values corresponding to reduction of $[N_3]$ ligands by

(41) Ogasawara, M.; Maseras, F.; Gallego-Planas, N.; Kawamura, K.; Ito, K.; Toyota, K.; Streib, W. E.; Komiya, S.; Eisenstein, O.; Caulton, K. G. *Organometallics* **1997**, *16*, 1979–1993.

(42) (a) Chung, M.; Ferguson, G.; Robertson, V.; Schlaf, M. *Can. J. Chem.* **2001**, *79*, 949–957. (b) Olmstead, M. M.; Maisonnat, A.; Farr, J. P.; Balch, A. L. *Inorg. Chem.* **1981**, *20*, 4060–4064.

(43) (a) Werner, H.; Tena, M. A.; Mahr, N.; Peters, K.; von Schnering, H. *Chem. Ber.* **1995**, *128*, 41–47. (b) Esteruelas, M. A.; Werner, H. *J. Organomet. Chem.* **1986**, *303*, 221–231.

(44) Smith, J. M.; Lachicotte, R. J.; Pittard, K. A.; Cundari, T. R.; Lukat-Rodgers, G.; Rodgers, K. R.; Holland, P. L. *J. Am. Chem. Soc.* **2001**, *123*, 9222–9223.

Table 1. Selected $[\text{N}_3]$ Ligand Bond Distances (\AA) of $[\text{N}_3]\text{RuCl}_2(\text{PMe}_3)$, $[\text{N}_3]\text{RuCl}_2(\text{CO})$, **2a**, **3c**, **5a**, **6a**, and **7a**^a

| bond | $[\text{N}_3^{\text{xy}1}]$ | $[\text{N}_3]\text{RuCl}_2(\text{PMe}_3)$ | $[\text{N}_3]\text{RuCl}_2(\text{CO})$ | 2a | 3c | 5a | 6a | 7a |
|-----------------------------|-----------------------------|---|--|---------------------|-----------|-----------|-----------|-----------|
| Ru– N_{im} | | 2.119(3); | 2.119(2); | 1.985(2); | 2.014(5); | 2.065(2); | 2.067(2); | 2.091(3); |
| C=N | 1.268(2) | 1.313(4); | 1.301(3); | 1.344(3), 1.282(3); | 1.359(7); | 1.352(3); | 1.334(3); | 1.348(5); |
| C– C_{pyr} | 1.495(2) | 1.466(5); | 1.478(4); | 1.397(3), 1.491(3); | 1.432(8); | 1.420(3); | 1.420(3); | 1.418(5); |
| Ru– N_{pyr} | | 1.971(3); | 2.006(2); | 2.032(2); | 1.942(7); | 1.971(2); | 1.947(2); | 1.964(3); |

^a Numbers in parentheses are estimated standard deviations in the least significant digits. Chemically equivalent distances are averaged.

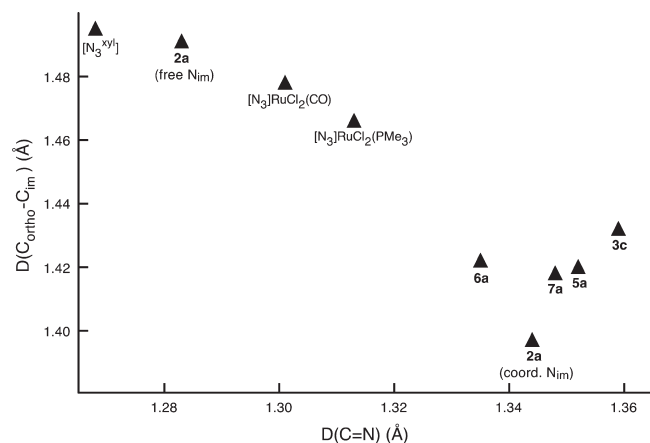


Figure 8. Comparison of the bond distances in $[\text{N}_3]\text{Ru}$ complexes and the free ligand, $[\text{N}_3^{\text{xy}1}]$.⁴⁵ Chemically equivalent distances are averaged.

one electron ($D(\text{C}=\text{N}) \approx 1.32 \text{ \AA}$, $D(\text{C}-\text{C}) \approx 1.44 \text{ \AA}$) and two electrons (1.36, 1.40 \AA), although again it is not clear if one can use metrical parameters to practically distinguish between the electron transfer implied by noninnocent valence tautomers and more classical metal-imine (or diimine) back-bonding. Values for the ruthenium complexes are summarized in Table 1 and in Figure 8. For comparison, the structurally characterized free $[\text{N}_3^{\text{xy}1}]$ ligand has also been included.⁴⁵ The coordinated and free imine groups of the bidentate $[\text{N}_3]$ complex **2a** are listed individually.

One primary trend emerges: the $\text{C}=\text{N}$ bonds lengthen, and the $\text{C}_{\text{pyr}}-\text{C}_{\text{im}}$ bonds contract on going from the free ligand to the $\text{Ru}(\text{II})$ complexes to the formally $\text{Ru}(0)$ complexes, consistent with increasing electronic delocalization into the $[\text{N}_3]$ ligand via π -back-bonding and/or contribution from a reduced-ligand tautomer (Scheme 2). The bidentate $\text{Ru}(0)$ complex **2** shows the greatest diversity of distances. There is reasonable agreement between the distances in the uncoordinated imine in **2** and the free ligand ($D(\text{C}=\text{N}) = 1.282(3)$ versus $1.268(2) \text{ \AA}$; $D(\text{C}-\text{C}) = 1.491(3)$ versus $1.495(2) \text{ \AA}$). The coordinated imine in **2** exhibits the shortest $\text{C}_{\text{pyr}}-\text{C}_{\text{im}}$ distance of all the complexes ($1.397(3) \text{ \AA}$), and correspondingly, the coordinated $\text{C}=\text{N}$ distance in **2** is fairly long ($1.344(3) \text{ \AA}$), although not as exceptional within the series as is the $\text{C}-\text{C}$ distance. Bidentate **2** is an interesting case—and not particularly representative of the other reduced $[\text{N}_3]\text{Ru}$ complexes—in that only the coordinated imine is in conjugation with the pyridine, with the free imine oriented out of the pyridine plane (torsional angle = 55°). As such, the conjugated system available to accommodate electron density from Ru is substantially smaller than in a tridentate $[\text{N}_3]$ ligand, and non-innocent valence tautomers (i.e., $[\text{N}_3]^-$ and $[\text{N}_3]^{2-}$) might be expected to be less favorable. On the other

hand, the effect of charge delocalization will be manifest on bond distances in only one imine, rather than spread over two, and hence more may appear more dramatic.

Although all of the formally $\text{Ru}(0)$ complexes exhibit longer $\text{C}=\text{N}$ and shorter $\text{C}_{\text{pyr}}-\text{C}_{\text{im}}$ distances than the formally $\text{Ru}(\text{II})$ species, no consistent trends are apparent, despite the large variation in π -acidity of co-ligands (N_2 , $(\text{PMe}_3)_2$, $(\text{PMe}_3)(\text{CO})$, and $(\text{CO})_2$). The nitrogen complex **3c** does exhibit the longest $\text{C}=\text{N}$ distances, and the average of $1.359(7) \text{ \AA}$ is nearly in the range suggested as for $[\text{N}_3]^{2-}/\text{Ru}(\text{II})$.^{38c} However, it should also be noted that the $\text{C}=\text{N}$ and $\text{C}-\text{C}$ distances in dicarbonyl **6a** ($1.335(3)$ and $1.422(4) \text{ \AA}$) are extremely similar to those in Chirik's iron analogue, $[\text{IPr}]\text{Fe}(\text{CO})_2$ ($1.333(2)$ and $1.424(2) \text{ \AA}$.) Given the similar ligand metrical parameters and nearly identical CO stretching frequencies (vide supra), it seems reasonable that the same formalism should be used to describe both the iron and ruthenium dicarbonyl complexes. On the one hand, the $\text{C}=\text{N}$ and $\text{C}-\text{C}$ distances fall between the values suggested for $1e^-$ and $2e^-$ reduction of the $[\text{N}_3]$ ligands. On the other hand, the Mössbauer data and broken symmetry DFT calculations are consistent with the neutral $[\text{N}_3]/\text{Fe}(0)$ formulation of $[\text{N}_3]\text{Fe}(\text{CO})_2$.²² We suggest the analogous—and “innocent”—view of complex **6a** as formally $\text{Ru}(0)$ remains appropriate and descriptive.

Conclusions

A new class of low-valent ruthenium complexes containing 2,6-bis(imino)pyridyl ligands has been prepared, and these labile complexes serve as versatile reagents for the synthesis of a variety of $\text{Ru}(0)$ and $\text{Ru}(\text{II})$ complexes. The $[\text{N}_3]$ ligand provides tunable steric protection of the metal center, but also can serve as a hemilabile ligand able to reversibly dissociate an imine group. The $16e^-$ complex **3c** is the first structurally characterized $\text{Ru}(0)$ dinitrogen complex and also exhibits a square-planar geometry that is unusual for $\text{Ru}(0)$.

Overall, it can be concluded that electron delocalization into the bis(imino)pyridyl ligand reduces electron density at the metal in the formally $\text{Ru}(0)$ complexes, but probably not to the extent implied by the valence tautomeric $[\text{N}_3]^{2-}/\text{Ru}(\text{II})$ canonical form. Although the $[\text{N}_3]^-/\text{Ru}(\text{I})$ representation may portray the electron distribution more accurately than “ $\text{Ru}(0)$ ”, the suggested odd electron count on both ligand and metal—with antiferromagnetic coupling to yield net diamagnetism—is cumbersome and provides little predictive value for $[\text{N}_3]\text{Ru}$ complexes with strong-field co-ligands such as CO and PMe_3 . Application of Occam's Razor, or perhaps more appropriately the “Duck Test”,⁴⁶ suggests the $\text{Ru}(0)$ formalism is appropriate for these five-coordinate compounds. We note in closing, however, that the metalloradical

(45) Huang, Y.; Ma, X.; Zheng, S.; Chen, J.; Wei, C. *Acta Crystallogr., Sect. E: Struct. Rep. Online* **2006**, *62*, o3044–o3045.

(46) (a) “If it looks like a duck, swims like a duck, and quacks like a duck, then it probably is a duck.” (b) Hecht-Nielsen, R. *Neural Networks* **2005**, *18*, 111–115.

character implied by the $[\text{N}_3]^-/\text{Ru}(\text{I})$ formalism may prove helpful in understanding the observation that the four-coordinate dinitrogen complex **3** reacts with hydrogen to yield paramagnetic monohydride species, as will be detailed in a forthcoming report.⁴⁷ Regardless of the exact distribution of electron density between the metal and ligands, it is clear that bis(imino)pyridyl ligands allow access to reduced complexes that maintain the reactivity implied by the “Ru(0)” formalism. The electronic and geometrical flexibility of these bis(imino)pyridine ruthenium complexes should prove useful in the development of new catalysts and bond-forming processes. Reactions of **2** and **3** with hydrogen, silanes, alkynes, and other substrates, along with initial DFT calculations on this system, will be described in subsequent reports.

Experimental Section

All manipulations were performed in Schlenk-type glassware on a dual-manifold Schlenk line or a nitrogen-filled Vacuum Atmospheres glovebox.⁴⁸ ^1H NMR spectra were obtained at 300, 360, and 500 MHz on Bruker DMX-300, AM-360, and AMX-500 FT NMR spectrometers, respectively. ^2H NMR spectra were obtained at 76.8 MHz on a Bruker AM-500 spectrometer. $^{31}\text{P}\{^1\text{H}\}$ NMR spectra were recorded with broadband ^1H decoupling at 121.5 MHz on a Bruker DMX-300 spectrometer. $^{13}\text{C}\{^1\text{H}\}$ NMR spectra were obtained at 125.8 MHz on an AMX-500 NMR spectrometer. All NMR spectra were recorded at 303 K unless stated otherwise. Chemical shifts are reported relative to tetramethylsilane for ^1H and ^{13}C spectra and external 85% H_3PO_4 for ^{31}P resonances. The temperature of the NMR probe was calibrated against methanol (estimated error 0.3 K). Infrared spectra were recorded on a Perkin-Elmer model 1430 spectrometer. HRMS was acquired on an AutoSpec (Micromass) with chemical ionization (CH_4). Elemental analyses were performed by Robertson Laboratory, Inc. (Madison, NJ).

Hydrocarbon solvents were dried over Na/K alloy-benzophenone. Benzene- d_6 , toluene- d_8 , cyclohexane- d_{12} , and tetrahydrofuran- d_8 were dried over Na/K alloy. Chloroform- d was dried over molecular sieves. CO and C_2H_4 (Airco) were used as received. $[\text{Ru}(p\text{-cymene})\text{Cl}_2]_2$,⁴⁹ $[\text{N}_3^{\text{xy}}]_2$,² $[\text{Bu-N}_3^{\text{mes}}]$,⁵⁰ $[\text{N}_3^{\text{xy}}]\text{-RuCl}_2(\text{C}_2\text{H}_4)$,¹¹ $[\text{Bu-N}_3^{\text{mes}}]\text{-RuCl}_2(\text{C}_2\text{H}_4)$, and PMe_3 ⁵¹ were synthesized according to the literature procedures. HSiMe_3 was prepared by the reaction of Me_3SiCl and LiAlH_4 in $^n\text{Bu}_2\text{O}$ and purified by trap-to-trap vacuum fractionation. Triethylsilane (Aldrich) was dried over Na prior to use.

Synthesis of $[\text{N}_3^{\text{xy}}]\text{RuCl}_2(\text{PMe}_3)$. PMe_3 (328 mg, 4.31 mmol) was vacuum transferred into a solution of toluene (5 mL) and $[\text{N}_3^{\text{xy}}]\text{RuCl}_2(\text{C}_2\text{H}_4)$ (**1a**) (114 mg, 0.200 mmol). The solution was stirred for two days at room temperature. Volatiles were removed in vacuo, and the residue was recrystallized from 2:1 pentane/toluene at 0 °C, yielding 107 mg of air-stable purple $[\text{N}_3^{\text{xy}}]\text{RuCl}_2(\text{PMe}_3)$ (87% yield). ^1H NMR (benzene- d_6): δ 7.03 (d, $^3J_{\text{HH}} = 8.0$ Hz, 2H, Py- H_m), 6.88 (m, 7H, Xyl- $H_{m,p}$, Py- H_p), 2.40 (s, 12H, Xyl- Me), 1.93 (s, 6H, Im- Me), 1.08 (d, $^2J_{\text{PH}} = 8.5$ Hz, 9H, PMe_3). $^{13}\text{C}\{^1\text{H}\}$ NMR (benzene- d_6): δ 173.80 (s, 2C, C=N), 159.91 (s, 2C, Py- C_o), 151.68 (s, 2C, Xyl- $C-N$), 132.15, 129.58, 129.40, 126.40, and 123.15 (s, 13C, aryl C), 21.73 (s, 4C,

Xyl- Me), 17.61 (s, 2C, Im- Me), 15.22 (d, $^1J_{\text{PC}} = 24.7$ Hz, 3C, PMe_3). $^{31}\text{P}\{^1\text{H}\}$ NMR (toluene- d_8): δ -5.77 (s, 1P, PMe_3). Anal. Calcd for $\text{C}_{28}\text{H}_{36}\text{N}_3\text{PCl}_2\text{Ru}$: C, 54.45; H, 5.88; N, 6.80. Found: C, 54.56; H, 6.18; N, 6.61.

Synthesis of $[\text{N}_3^{\text{xy}}]\text{RuCl}_2(\text{CO})$. A CH_2Cl_2 solution (40 mL) of $[\text{N}_3^{\text{xy}}]\text{RuCl}_2(\text{C}_2\text{H}_4)$ (**1a**) (60 mg, 0.105 mmol) was stirred under CO (1 atm) for 45 min at room temperature, during which time the color of the reaction mixture changed from purple to red. Volatiles were removed in vacuo, and the residue was washed with C_6H_6 and filtered in air, yielding 50 mg of air-stable burgundy solid (83% yield). ^1H NMR (chloroform- d): δ 8.09 (t, $^3J_{\text{HH}} = 8.1$ Hz, 1H, Py- H_p), 7.94 (d, $^3J_{\text{HH}} = 8.0$ Hz, 2H, Py- H_m), 7.04 (m, 6H, Xyl- $H_{m,p}$), 2.46 (s, 6H, Im- Me), 2.29 (s, 12H, Xyl- Me). $^{13}\text{C}\{^1\text{H}\}$ NMR (chloroform- d): δ 202.51 (s, 1C, CO), 174.52 (s, 2C, C=N), 157.49 (s, 2C, Py- C_o), 148.90 (s, 2C, Xyl- $C-N$), 138.37, 130.39, 129.24, 127.00, and 124.72 (s, 13C, aryl C), 20.91 (s, 4C, Xyl- Me), 18.98 (s, 2C, Im- Me). IR (Nujol): $\nu(\text{CO}) = 1963$ cm^{-1} . HRMS (ES): calcd 592.047 (M^{102}Ru) + Na^+ , found 592.0491; calcd 594.047 (M^{104}Ru) + Na^+ , found 594.0478.

Synthesis of $[\kappa^2\text{-N}_3^{\text{xy}}]\text{Ru}(\eta^6\text{-MeC}_6\text{H}_5)$, **2a.** A toluene solution (35 mL) of $[\text{N}_3^{\text{xy}}]\text{RuCl}_2(\text{C}_2\text{H}_4)$ (**1a**) (1.00 g, 0.00176 mol) and Et_3SiH (1.7 mL, 1.22 g, 0.0105 mol) was stirred under nitrogen for 16 h at room temperature. The reaction mixture was then reduced in volume to approximately 5 mL in vacuo. The product was recrystallized from 2:1 pentane/toluene at -78 °C, yielding 0.770 g of purple **2a** (78% yield). ^1H NMR (toluene- d_8): δ 6.98 and 6.63 (m, 9H, aryl H), 5.10 (t, $^3J_{\text{HH}} = 5.4$ Hz, 1H, Tol- H_p), 4.56 (t, $^3J_{\text{HH}} = 5.5$ Hz, 2H, Tol- H_m), 4.29 (d, $^3J_{\text{HH}} = 5.5$ Hz, 2H, Tol- H_o), 2.39 (s, 3H, Im- Me), 2.34 (s, 6H, Xyl- Me), 1.98 (s, 6H, Xyl- Me), 1.66 (s, 3H, Im- Me), 1.60 (s, 3H, Tol- Me). $^{13}\text{C}\{^1\text{H}\}$ NMR (toluene- d_8): δ 170.05 (s, 1C, C=N), 165.50 (s, 1C, C=N), 162.85 (s, 1C, Py- C_o), 155.02 (s, 1C, Py- C_o), 148.84 (s, 1C, Xyl- $C-N$), 146.02 (s, 1C, Xyl- $C-N$), 129.32, 129.30, 128.95, 128.51, 128.30, 128.13, 125.66, 125.25, 125.04, 123.51, 118.65, 116.98 (s, 19C, aryl C), 21.39 (s, 1C, Tol- Me), 19.66 (s, 1C, Im- Me), 18.83 (s, 2C, Xyl- Me), 18.25 (s, 2C, Xyl- Me), 14.24 (s, 1C, Im- Me). Anal. Calcd for $\text{C}_{32}\text{H}_{35}\text{N}_3\text{Ru}$: C, 68.30; H, 6.27; N, 7.46. Found: C, 68.40; H, 6.15; N, 7.15.

$[\kappa^2\text{-N}_3^{\text{mes}}]\text{Ru}(\eta^6\text{-MeC}_6\text{H}_5)$, **2b.** A toluene solution (30 mL) of $[\text{N}_3]\text{RuCl}_2(\text{C}_2\text{H}_4)$ (**1b**), (1.08 g, 0.0018 mol), and Et_3SiH (1.8 mL, 1.22 g, 0.0111 mol) was stirred under nitrogen for 16 h at room temperature. The reaction mixture was then reduced in volume to approximately 5 mL in vacuo. The product was recrystallized from 2:1 pentane/toluene at -78 °C using a swivel frit under inert conditions, yielding 0.700 g of purple **2b** (66% yield). ^1H NMR (toluene- d_8): δ 7.06, 6.88, and 6.65 (m, 7H, aryl H), 5.15 (t, $^3J_{\text{HH}} = 5.4$ Hz, 1H, Tol- H_p), 4.59 (t, $^3J_{\text{HH}} = 5.4$ Hz, 2H, Tol- H_m), 4.35 (d, $^3J_{\text{HH}} = 5.4$ Hz, 2H, Tol- H_o), 2.43 (s, 3H, Im- Me), 2.34 (s, 6H, Mes- Me_o), 2.29 and 2.26 (s, each 3H, Mes- Me_p), 1.99 (s, 6H, Mes- Me_o), 1.70 (s, 3H, Im- Me), 1.66 (s, 3H, Tol- Me).

$[\kappa^2\text{-Bu-N}_3^{\text{mes}}]\text{Ru}(\eta^6\text{-MeC}_6\text{H}_5)$, **2c.** A toluene solution (7 mL) of $[\text{Bu-N}_3^{\text{mes}}]\text{RuCl}_2(\text{C}_2\text{H}_4)$ (**1c**) (200 mg, 0.306 mmol) and Et_3SiH (0.3 mL, 0.216 g, 1.846 mmol) was stirred under nitrogen for 20 h at room temperature. The reaction mixture was then reduced in volume to approximately 2 mL in vacuo. The product was recrystallized from 2:1 pentane/toluene at -78 °C, yielding 166.5 mg of purple **2c** (84% yield). ^1H NMR (toluene- d_8): δ 7.26 (s, 2H, Py- H_m), 6.89 (s, 4H, Mes- H_m), 5.18 (t, $^3J_{\text{HH}} = 5.2$ Hz, 1H, Tol- H_p), 4.61 (t, $^3J_{\text{HH}} = 5.4$ Hz, 2H, Tol- H_m), 4.37 (d, $^3J_{\text{HH}} = 5.4$ Hz, 2H, Tol- H_o), 2.45 (s, 3H, Im- Me), 2.39 (s, 6H, Mes- Me_o), 2.30 (s, 3H, Mes- Me_p), 2.27 (s, 3H, Mes- Me_p), 2.16 (s, 3H, Im- Me), 2.05 (s, 6H, Mes- Me_o), 1.82 (s, 3H, Im- Me), 1.24 (s, 9H, ^tBu).

Observation of $[\text{N}_3^{\text{xy}}]\text{Ru}(\text{H})(\text{Cl})(\text{C}_2\text{H}_4)$. A NMR tube was loaded with a toluene- d_8 solution (0.3 mL) of $[\text{N}_3^{\text{xy}}]\text{RuCl}_2(\text{C}_2\text{H}_4)$ (**1a**) (10 mg, 0.0176 mmol) and Et_3SiH (25 μL , 0.155 mmol) under nitrogen. The reaction was monitored by ^1H NMR spectroscopy. After 30 min at room temperature, the solution contained a mixture of $[\text{N}_3^{\text{xy}}]\text{Ru}(\text{H})(\text{Cl})(\text{C}_2\text{H}_4)$ (ca. 68%) and

(47) Wieder, N. L.; Gallagher, M.; Carroll, P. J.; Berry, D. H. To be submitted.

(48) *Experimental Organometallic Chemistry*; Wayda, A. L., Darensbourg, M. Y., Eds.; American Chemical Society: Washington, D.C., 1987.

(49) Bennett, M. A.; Huang, T. N.; Matheson, T. W.; Smith, A. K. *Inorg. Synth.* **1982**, *21*, 74–78.

(50) Nüchel, S.; Burger, P. *Organometallics* **2001**, *20*, 4345–4359.

(51) Luetkens, M. L.; Sattelberger, A. P.; Murray, H. H.; Basil, J. D.; Fackler, J. P. *Inorg. Synth.* **1989**, *26*, 7–12.

2a (ca. 32%). Et_3SiCl , Et_4Si , and CH_3CH_3 were also observed. ^1H NMR (toluene- d_8): δ 6.90 (m, 9H, aryl *H*), 4.12 (s, 4H, C_2H_4), 2.51 (s, 6H, *Im-Me*), 1.89 (s, 6H, *Xyl-Me*), 1.73 (s, 6H, *Xyl-Me*), –2.91 (s, 1H, *Ru-H*).

Synthesis of $[\text{N}_3^{\text{xy}}]\text{Ru}(\text{H})(\text{Cl})(\text{PMe}_3)$. A toluene solution (3 mL) of $[\text{N}_3^{\text{xy}}]\text{RuCl}_2(\text{PMe}_3)$ (**1b**) (85 mg, 0.138 mmol) and Et_3SiH (350 μL , 2.16 mmol) was added to a 100 mL thick-walled pressure flask under nitrogen. The purple solution was heated to 150 °C for 3.5 h, during which time the color changed to red. Volatiles were removed in vacuo, and the product was recrystallized from 2:1 pentane/toluene at –78 °C, yielding 48 mg of red powder (60% yield). ^1H NMR (toluene- d_8): δ 6.90 (m, 9H, aryl *H*), 2.51 (s, 6H, *Im-Me*), 1.84 (s, 6H, *Xyl-Me*), 1.82 (s, 6H, *Xyl-Me*), 0.83 (d, $^2J_{\text{PH}} = 7.4$ Hz, 9H, PMe_3), –19.17 (d, $^2J_{\text{PH}} = 42.5$ Hz, 1H, *RuH*). $^{13}\text{C}\{^1\text{H}\}$ NMR (toluene- d_8): δ 165.77 (s, 2C, C=N), 157.60 (s, 2C, Py-C_o), 153.10 (s, 2C, *Xyl-C-N*), 129.63, 129.12, 128.64, 125.93, 125.81, 119.30, and 119.19 (s, 13C, aryl *C*), 18.08 (d, $^1J_{\text{PC}} = 23.8$ Hz, 3C, PMe_3), 20.49 and 18.62 (s, 4C, *Xyl-Me*), 16.33 (s, 2C, *Im-C*). $^{31}\text{P}\{^1\text{H}\}$ NMR (toluene- d_8): –4.25 (s, 1P, PMe_3).

Synthesis of $[\text{N}_3^{\text{xy}}]\text{Ru}_2(\mu\text{-N}_2)$, **3a.** $[\kappa^2\text{-N}_3^{\text{xy}}]\text{Ru}(\eta^6\text{-MeC}_6\text{H}_5)$ (**2a**) (215 mg, 0.382 mmol) was loaded into a 100 mL round-bottom flask under N_2 (1 atm) in cyclohexane (8 mL). The purple slurry was stirred at room temperature for 2 days and periodically exposed to fresh N_2 . The color gradually became dark blue. The product was isolated by filtration under N_2 and residual **2a** removed by washing with cyclohexane until the filtrate became turquoise in color. The resulting turquoise solid was dried in vacuo, yielding 165 mg of **3a** (89% yield). Small solid samples of **3a** spontaneously enflame upon exposure to air. ^1H NMR (cyclohexane- d_{12}): δ 8.59 (t, $^3J_{\text{HH}} = 7.4$ Hz, 2H, Py-H_m), 8.12 (d, $^3J_{\text{HH}} = 7.4$ Hz, 4H, Py-H_m), 6.79 (d, $^3J_{\text{HH}} = 7.4$ Hz, 8H, *Xyl-H_m*), 6.57 (t, $^3J_{\text{HH}} = 7.4$ Hz, 4H, *Xyl-H_p*), 1.81 (s, 24H, *Xyl-Me*), –0.08 (s, 12H, *Im-Me*). $^{13}\text{C}\{^1\text{H}\}$ NMR (tetrahydrofuran- d_8): δ 158.00 (s, 4C, C=N), 157.36 (s, 4C, Py-C_o), 156.16 (s, 4C, *Xyl-C-N*), 130.16, 128.61, 124.94, 124.59, and 114.41 (s, 26C, aryl *C*), 20.84 (s, 8C, *Xyl-Me*), 19.86 (s, 4C, *Im-Me*). IR (Nujol): 1856 cm^{-1} (w), tentatively assigned as $\nu(\text{NN})$.

$[\text{N}_3^{\text{mes}}]\text{Ru}_2(\mu\text{-N}_2)$, **3b**. A round-bottomed flask was charged with $[\kappa^2\text{-N}_3^{\text{mes}}]\text{Ru}(\eta^6\text{-MeC}_6\text{H}_5)$ (**2b**) (100 mg, 0.169 mmol) and decane (25 mL). The resultant slurry was stirred under 1 atm of N_2 until the color of the solution changed from purple to turquoise. The volume of the solution was then reduced in vacuo by ca. 50% in an attempt to reduce the amount of free toluene, and the slurry was again stirred under 1 atm N_2 until the solution changed to turquoise again, indicating displacement of coordinated toluene by N_2 . The process was repeated twice, or until the color of the solution remained turquoise upon stirring under vacuum. The slurry was then filtered to collect the solid, and the solid was washed with hexanes to afford 22 mg of **3b** (25% yield). Note: the $[\text{N}_3^{\text{mes}}]$ ligand imparts greater solubility to **3b**, reducing the yield of solid collected in this manner. Additional crops of **3b** contaminated with varying amounts of **2b**, but suitable for preparative reactions, can also be recovered. ^1H NMR (cyclohexane- d_{12}): δ 8.58 (t, $^3J_{\text{HH}} = 7.9$ Hz, 2H, Py-H_p), 8.10 (d, $^3J_{\text{HH}} = 7.9$ Hz, 4H, Py-H_m), 6.60 (s, 8H, *Mes-H_m*), 1.97 (s, 12H, *Mes-Me_p*), 1.75 (s, 24H, *Mes-Me_o*), –0.05 (s, 12H, *Im-Me*). UV-vis: $\lambda_{\text{max}} = 638$ nm, $\epsilon = 11\,900$.

$[\text{Bu-N}_3^{\text{mes}}]\text{Ru}_2(\mu\text{-N}_2)$, **3c**. $[\kappa^2\text{-Bu-N}_3^{\text{mes}}]\text{Ru}(\eta^6\text{-MeC}_6\text{H}_5)$ (**2c**) (166.5 mg, 0.258 mmol) was loaded into a 100 mL round-bottom flask under N_2 (1 atm) in cyclohexane (5 mL). The purple slurry was stirred at room temperature for 2 days and periodically exposed to fresh N_2 . The color gradually became dark blue. The product was isolated by filtration under N_2 and residual **2c** removed by washing with cyclohexane until the filtrate became turquoise in color. The resulting turquoise solid was dried in vacuo, yielding 87 mg of **3c** (57% yield). ^1H NMR (cyclohexane- d_{12}): δ 8.25 (s, 4H, Py-H_m), 6.59 (s, 8H, *Mes-H_m*), 1.97 (s, 12H, *Mes-Me_p*), 1.75 (s, 24H, *Mes-Me_o*), 1.29 (s, 18H, *Bu*), –0.09 (s, 12H, *Im-Me*).

Observation of $[\text{N}_3^{\text{xy}}]\text{Ru}(\text{C}_2\text{H}_4)_2$ **4a.** A NMR tube sample of $[\kappa^2\text{-N}_3^{\text{xy}}]\text{Ru}(\eta^6\text{-MeC}_6\text{H}_5)$ (**2a**) (4 mg, 0.00711 mmol) in cyclohexane- d_{12} (0.3 mL) was flame-sealed under 1 atm of C_2H_4 at –196 °C. Upon warming to room temperature, the reaction mixture changed from purple to burgundy in 5 min. The resulting ^1H NMR spectrum showed complete conversion of **2a** to **4a**, with the concurrent release of toluene. The reaction mixture decomposed during attempts to remove the volatiles in vacuo or recrystallize the product. ^1H NMR (cyclohexane- d_{12}): δ 7.99 (d, $^3J_{\text{HH}} = 7.6$ Hz, 2H, Py-H_m), 7.32 (t, $^3J_{\text{HH}} = 7.4$ Hz, 1H, Py-H_p), 6.93 (d, $^3J_{\text{HH}} = 7.5$ Hz, 4H, *Xyl-H_m*), 6.86 (t, $^3J_{\text{HH}} = 7.5$ Hz, 2H, *Xyl-H_p*), 2.28 (s, 6H, *Im-Me*), 1.76 (s, 12H, *Xyl-Me*), 1.63 (s, 8H, C_2H_4). $^{13}\text{C}\{^1\text{H}\}$ NMR (cyclohexane- d_{12}): δ 155.82 (s, 2C, C=N), 150.38 (s, 2C, Py-C_o), 146.90 (s, 2C, *Xyl-C-N*), 130.25 (s, 1C, Py-C_p), 128.74 (s, 2C, *Xyl-C_p*), 125.20 and 123.04 (s, 8C, *Xyl-C_{o,m}*), 117.28 (s, 2C, Py-C_o), 59.00 (s, 4C, C_2H_4), 18.94 (s, 4C, *Xyl-Me*), 16.31 (s, 2C, *Im-Me*).

Synthesis of $[\text{N}_3^{\text{xy}}]\text{Ru}(\text{PMe}_3)_2$, **5a.** PMe_3 (73.20 mg, 0.962 mmol) was added by vacuum transfer to a toluene solution (5 mL) of $[\kappa^2\text{-N}_3^{\text{xy}}]\text{Ru}(\eta^6\text{-MeC}_6\text{H}_5)$ (**2a**) (60 mg, 0.107 mmol) at –196 °C. Upon warming to room temperature, a color change from purple to red was observed within seconds. The reaction mixture was stirred for 30 min, and volatiles were removed in vacuo. The red product was recrystallized from pentane at –78 °C, yielding 57 mg of **5a** (86%). ^1H NMR (toluene- d_8): δ 8.08 (d, $^3J_{\text{HH}} = 7.6$ Hz, 2H, Py-H_m), 7.25 (t, $^3J_{\text{HH}} = 7.6$ Hz, 1H, Py-H_p), 6.94 (m, 6H, *Xyl-H_{m,p}*), 2.28 (s, 6H, *Im-Me*), 1.72 (br s, 12H, *Xyl-Me*), 0.52 (d, $^2J_{\text{PH}} = 7.5$ Hz, 18H, PMe_3). $^{13}\text{C}\{^1\text{H}\}$ NMR (benzene- d_6): δ 157.42 (s, 2C, C=N), 144.91 (s, 2C, Py-C_o), 143.90 (s, 2C, *Xyl-C-N*), 131.44 (s, 1C, Py-C_p), 129.43 (s, 2C, *Xyl-C_p*), 124.50 and 118.18 (s, 8C, *Xyl-C_{o,m}*), 114.29 (s, 2C, Py-C_m), 20.36 (s, 4C, *Xyl-Me*), 18.75 (d, $^1J_{\text{PC}} = 21.9$ Hz, 6C, PMe_3), 15.98 (s, 2C, *Im-Me*). $^{31}\text{P}\{^1\text{H}\}$ NMR (toluene- d_8): δ 4.83 (br s, 2P, PMe_3).

VT ^1H NMR of $[\text{N}_3^{\text{xy}}]\text{Ru}(\text{PMe}_3)_2$, **5a.** ^1H NMR (toluene- d_8 , 198 K): δ 8.07 (d, $^3J_{\text{HH}} = 7.5$ Hz, 2H, Py-H_m), 7.29 (t, $^3J_{\text{HH}} = 7.6$ Hz, 1H, Py-H_p), 6.93 (m, 6H, *Xyl-H_{m,p}*), 2.30 (s, 6H, *Im-Me*), 1.85 (s, 6H, *Xyl-Me*), 1.48 (s, 6H, *Xyl-Me*), 0.77 (d, $^2J_{\text{PH}} = 4.2$ Hz, 9H, PMe_3), 0.24 (d, $^2J_{\text{PH}} = 8.2$ Hz, 9H, PMe_3); (toluene- d_8 , 228 K): δ 8.07 (d, $^3J_{\text{HH}} = 7.5$ Hz, 2H, Py-H_m), 7.28 (t, $^3J_{\text{HH}} = 7.6$ Hz, 1H, Py-H_p), 6.95 (m, 6H, *Xyl-H_{m,p}*), 2.30 (s, 6H, *Im-Me*), 1.85 (s, 6H, *Xyl-Me*), 1.48 (s, 6H, *Xyl-Me*), 0.74 (d, $^2J_{\text{PH}} = 4.2$ Hz, 9H, PMe_3), 0.29 (d, $^2J_{\text{PH}} = 8.2$ Hz, 9H, PMe_3); (toluene- d_8 , 237 K): δ 8.07 (d, $^3J_{\text{HH}} = 7.2$ Hz, 2H, Py-H_m), 7.27 (t, $^3J_{\text{HH}} = 7.6$ Hz, 1H, Py-H_p), 6.95 (m, 6H, *Xyl-H_{m,p}*), 2.29 (s, 6H, *Im-Me*), 1.85 (s, 6H, *Xyl-Me*), 1.48 (s, 6H, *Xyl-Me*), 0.54 (br, 18H, PMe_3); (toluene- d_8 , 263 K): δ 8.06 (d, $^3J_{\text{HH}} = 7.5$ Hz, 2H, Py-H_m), 7.27 (t, $^3J_{\text{HH}} = 7.6$ Hz, 1H, Py-H_p), 6.95 (m, 6H, *Xyl-H_{m,p}*), 2.28 (s, 6H, *Im-Me*), 1.71 (br s, 12H, *Xyl-Me*), 0.50 (br, 18H, PMe_3). $^{31}\text{P}\{^1\text{H}\}$ NMR (toluene- d_8 , 198 K): δ 13.95 (d, $^2J_{\text{PP}} = 12.2$ Hz, 1P, PMe_3), –3.16 (d, $^2J_{\text{PP}} = 13.3$ Hz, 1P, PMe_3); (toluene- d_8 , 228 K): δ 13.42 (br s, 1P, PMe_3), –3.40 (br s, 1P, PMe_3); (toluene- d_8 , 237 K): δ 13.42 (br s, 1P, PMe_3), –3.35 (br s, 1P, PMe_3); (toluene- d_8 , 263 K): δ 13 (vbr s, 1P, PMe_3), –2 (vbr s, 1P, PMe_3).

Reaction of $[\text{N}_3^{\text{xy}}]\text{Ru}(\text{PMe}_3)_2$ with $\text{PMe}_3\text{-}d_9$. A NMR tube was loaded with a benzene- d_6 solution (0.3 mL) of $[\text{N}_3^{\text{xy}}]\text{Ru}(\text{PMe}_3)_2$ (**5a**) (5 mg, 0.00804 mmol), and the solution was degassed in vacuo. $\text{PMe}_3\text{-}d_9$ (0.0243 mmol) was added by vacuum transfer, and the tube sealed with a torch. The attempted reaction was monitored periodically by ^1H and ^2H NMR for 4 weeks at room temperature. No exchange of $\text{PMe}_3\text{-}d_9$ with coordinated PMe_3 was observed.

Synthesis of $[\text{N}_3^{\text{xy}}]\text{Ru}(\text{CO})_2$, **6a.** A toluene solution (10 mL) of $[\kappa^2\text{-N}_3^{\text{xy}}]\text{Ru}(\eta^6\text{-MeC}_6\text{H}_5)$ (**2a**) (57 mg, 0.101 mmol) was placed in a swivel frit and stirred under CO (1 atm) for 20 min at room temperature, at which time the color changed from purple to green. The solvent was removed in vacuo, and the product was recrystallized from 3:1 pentane/toluene at –78 °C, yielding 42 mg of green **6a** (78% yield). ^1H NMR (benzene- d_6): δ 7.69

(d, $^3J_{\text{HH}} = 7.7$ Hz, 2H, Py- H_{m}), 6.98 (d, $^3J_{\text{HH}} = 7.5$ Hz, 4H, Xyl- H_{m}), 6.94 (m, 3H Py- H_{p} , Xyl- H_{p}), 2.09 (s, 6H, Im- Me), 1.99 (s, 12H, Xyl- Me). $^{13}\text{C}\{^1\text{H}\}$ NMR (benzene- d_6): δ 200.93 (s, 2C, CO), 153.89 (s, 2C, C=N), 153.61 (s, 2C, Py- C_{o}), 141.87 (s, 2C, Xyl-C-N), 129.74 (s, 1C, Py- C_{p}), 129.09 (s, 2C, Xyl- C_{p}), 126.17 and 124.19 (s, 8C, Xyl- $C_{\text{o,m}}$), 113.34 (s, 2C, Py- C_{m}), 18.57 (s, 4C, Xyl- Me), 15.02 (s, 2C, Im- Me). IR (Nujol): $\nu(\text{CO}) = 1925$, 1978 cm^{-1} .

Synthesis of $[\text{N}_3^{\text{xy}}]\text{Ru}(\text{PMe}_3)(\text{CO})$, **7a.** PMe_3 (33 mg, 0.433 mmol) was vacuum transferred into a benzene solution (3 mL) of $[\text{N}_3^{\text{xy}}]\text{Ru}(\text{CO})_2$ (**6a**) (46 mg, 0.0874 mmol) at -196°C . The mixture was thawed and stirred for 15 h at room temperature, during which time the color changed from green to orange. The volatiles were removed in vacuo, and the resulting residue was recrystallized from 2:1 pentane/toluene at -35°C , yielding 36 mg of **7a** (72% yield). ^1H NMR (benzene- d_6): δ 7.88 (d, $^3J_{\text{HH}} = 7.5$ Hz, 2H, Py- H_{m}), 6.95 (m, 7H, Xyl- $H_{\text{m,p}}$, Py- H_{p}), 2.25 (s, 6H, Im- Me), 2.21 (s, 6H, Xyl- Me), 1.60 (s, 6H, Xyl- Me), 0.63 (d, $^2J_{\text{PH}} = 7.9$ Hz, 9H, PMe_3). $^{13}\text{C}\{^1\text{H}\}$ NMR (benzene- d_6): δ 206.12 (d, $^2J_{\text{PC}} = 27.7$ Hz, 1C, CO), 155.44 (s, 2C, C=N), 150.44 (s, 2C, Py- C_{o}), 142.59 (s, 2C, Xyl-C-N), 131.74, 131.57, 129.48, 128.44, 125.43, 123.63, and 111.73 (s, 13C, aryl C), 19.09 (d, $^1J_{\text{PC}} = 14.2$ Hz, 3C, PMe_3), 18.95 (s, 4C, Xyl- Me), 15.34 (s, 2C, Im- Me). $^{31}\text{P}\{^1\text{H}\}$ NMR (benzene- d_6): δ 1.54 (s, 1P, PMe_3). IR (benzene): $\nu(\text{CO}) = 1963\text{ cm}^{-1}$.

Single-Crystal X-ray Diffraction Analyses. X-ray intensity data were collected on a Rigaku Mercury CCD area detector employing graphite-monochromated Mo $K\alpha$ radiation ($\lambda = 0.71069\text{ \AA}$) at a temperature of 143 K. Oscillation images were processed using CrystalClear,⁵² producing a listing of unaveraged F^2 and $\sigma(F^2)$ values, which were then passed to the Crystal Structure⁵³ program package for further processing. Refinement was by full-matrix least-squares based on F^2 using SHELXL-97.⁵⁴ All reflections were used during refinement (F^2 's that were experimentally negative were replaced by $F^2 = 0$). Non-hydrogen atoms were refined anisotropically, and hydrogen atoms were refined using a "riding" model and structure refinement. In all cases, non-hydrogen atoms were refined anisotropically and hydrogen atoms were refined using a "riding" model.

The dichloride carbonyl complex $[\text{N}_3^{\text{xy}}]\text{RuCl}_2(\text{CO})$ cocrystallized with one-half chlorobenzene molecule per unit cell. The chlorobenzene sits on an inversion center, with the pseudo-

centric structure resulting from a 1:1 disorder of 1- and 4-positions on the ring (Cl3 and H27).

In the case of nitrogen complex **3c**, a significant solvent-accessible void was observed in the unit cell, although relatively little electron density was observed in difference Fourier maps. Analysis using SQUEEZE⁵⁵ indicated the void is accommodating atoms containing only ca. 12 electrons. The small void size and low electron density are inconsistent with cocrystallized cyclohexane solvent, but the possibility of cocrystallized dinitrogen gas (14 electrons) was considered. Inspection of the packing diagram indicates that the void forms an infinite channel parallel to the c -axis. Although refinement including a full occupancy N_2 molecule did lead to a decrease in R_1 from 5.74% to ca. 4.9%, the atomic positions and thermal parameters of the " N_2 " were not well-behaved and were omitted from the final model. The residual electron density was accounted for in the final structure factor calculation using the SQUEEZE program. Nonbonded, cocrystallized dinitrogen is not common, but has been observed in several other instances.⁵⁶ Given that the voids form continuous channels through the crystal, it is also not surprising that the dinitrogen could be positionally disordered, or at only partial occupancy in the lattice, and hence difficult to model.

Acknowledgment. We are grateful to the National Science Foundation for support of this work under grant CHE-9904798. We also thank Andrew Blum for his assistance with the synthesis of the $[\text{Bu-N}_3^{\text{mes}}]$ ligand.

Supporting Information Available: X-ray crystallographic data (in CIF format) and ^1H NMR spectra of purified samples are available free of charge via the Internet at <http://pubs.acs.org>.

(55) SQUEEZE: Sluis, P. v.d.; Spek, A. L. *Acta Crystallogr.* **1990**, *A46*, 194.

(56) (a) Phillips, A. E.; Goodwin, A. L.; Halder, G. J.; Southon, P. D.; Kepert, C. J. *Angew. Chem., Int. Ed.* **2008**, *47*, 1369–1399. (b) Ma, X.; You, Z. *Transition Met. Chem.* **2008**, *33*, 961–965. (c) Kachi-Terajima, C.; Akatsuka, T.; Takamizawa, S. *Chem. Asian J.* **2007**, *2*, 40–50. (d) Makarov, A. Y.; Tersango, K.; Nivesanond, K.; Blockhuys, C. V. A.; Kovalev, M. K.; Bagryanskaya, I. Y.; Gatilov, Y. V.; Shakirov, M. M.; Zibarev, A. V. *Inorg. Chem.* **2006**, *45*, 2221–2228. (e) Rowsell, J. L. C.; Spencer, E. C.; Eckert, J.; Howard, J. A. K.; Yaghi, O. M. *Science* **2005**, *309*, 1350–1354. (f) Clarke, C. S.; Haynes, D. A.; Rawson, J. M.; Bond, A. D. *Chem. Commun.* **2003**, 2774–2775. (g) Bryan, C. D.; Cordes, A. W.; Haddon, R. C.; Hicks, R. G.; Kennepohl, D. K.; MacKinnon, C. D.; Oakley, R. T.; Palstra, T. M. M.; Perel, A. S.; Scott, S. R.; Schneemeyer, L. F.; Waszczak, J. V. *J. Am. Chem. Soc.* **1994**, *116*, 1205–1210. (h) Balch, A. L.; Olmstead, M. M.; Safari, N. J. *Inorg. Chem.* **1993**, *32*, 291–296. (i) Wood, F. E.; Olmstead, M. M.; Balch, A. L. *J. Am. Chem. Soc.* **1983**, *105*, 6332–6334. (j) Gies, H. Z. *Kristallogr. Kristallgem. Kristallphys. Kristallchem.* **1983**, *164*, 247–257.

(52) *CrystalClear*; Rigaku Corporation, **1999**.

(53) *Crystal Structure: Crystal Structure Analysis Package*; Rigaku Corporation, **2002**.

(54) Sheldrick, G. M. *SHELXL-97: Program for the Refinement of Crystal Structures*; University of Göttingen, Germany, 1997.